TURUN YLIOPISTON JULKAISUJA
ANNALES UNIVERSITATIS TURKUENSIS

SARJA - SER. A I OSA - TOM. 394

ASTRONOMICA - CHEMICA - PHYSICA - MATHEMATICA

EVOLUTION AND STELLAR CONTENT OF AGN HOST GALAXIES

by

Tomi Hyvönen

TURUN YLIOPISTO
Turku 2009

From the Department of Physics
University of Turku
Turku, Finland

Supervised by

Docent Jari Kotilainen
Tuorla Observatory
University of Turku
Turku, Finland

Reviewed by

PhD Ross McLure
Institute of Astronomy
University of Edinburgh
Edinburgh, United Kingdom

and

PhD Margrethe Wold
Institute of Theoretical Astrophysics
Oslo, Norway

Opponent

Dr Knud Jahnke
Max-Planck-Institute for Astronomy
Heidelberg, Germany

ISBN 978-951-29-3907-7 (PRINT)
ISBN 978-951-29-3908-4 (PDF)
ISSN 0082-7002
Painosalama Oy – Turku, Finland 2009

“We are all in the gutter, but some of us are looking at the stars.”

Oscar Wilde

Acknowledgements

I am grateful to numerous people who have made it possible for me to complete this thesis. First of all, I would like to thank my supervisor, Jari Kotilainen, for his precious counseling and guidance in the field of extragalactic astronomy. It has been a privilege for me to work with a person such as him. Another person I am grateful to is Juha Reunanen, who always helped me with his unlimited knowledge. At those days, especially, when I was struggling with near-infrared data reduction for the first time, his support was more than priceless. Furthermore, I would like to thank all the collaborators I have been able to work with.

Unfortunately, it is impossible to thank individually each and everyone who have generously offered help for me during these years. So I want to thank all the students and staff in Tuorla Observatory, which has offered me excellent and inspiring surroundings for my first steps in astronomical research. I would like, especially, to give credit to the Tuorla floorball team, and thank the team for helping me to keep in shape.

No matter how interesting work you have, without friends life would be just like empty space. I am grateful to my dear friends, Leena and Jani, who for all these years have shed light to my life like bright stars, and continuously supported me in my life. This work would not have been possible without you. Sincerely, thank you!

I also want to thank my dear brother, Mika, for inspiring discussions we have shared during these years. Last but not least, I want to thank my parents, Maria and Pentti, who have given their endless support for this project ever since I, at one sunny day, told them that I am going to move from Tampere to Turku to study astronomy.

Finally, for financial support, I would like to thank the Academy of Finland.

Contents

List of Figures

List of Publications

I *The luminous host galaxies of high redshift BL Lac objects*
Kotilainen, J.K., **Hyvönen, T**. & Falomo, R.
Astron. Astrophys., 440, 831-843 (2005)

II *The host galaxies of radio-quiet quasars at 0.5 < z < 1.0*
Hyvönen, T., Kotilainen, J.K., Örndahl, E., Falomo, R. & Uslenghi, M.
Astron. Astrophys., 462, 525-533 (2007)

III *The stellar content of low redshift BL Lacertae host galaxies from multicolor imaging*
Hyvönen, T., Kotilainen, J.K., Falomo, R., Örndahl, E. & Pursimo, T.
Astron. Astrophys., 476, 723-734 (2007)

IV *The stellar content of low redshift radio galaxies from near-infrared spectroscopy*
Hyvönen, T., Kotilainen, J.K., Reunanen, J. & Falomo, R.
Astron. Astrophys., accepted for publication (2009)

Abstract

In this dissertation, Active Galactic Nuclei (AGN) and their host galaxies are discussed. Together with transitional events, such as supernovae and gamma-ray bursts, AGN are the most energetic phenomena in the Universe. The dominant fraction of their luminosity originates from the center of a galaxy, where accreting gas falls into a supermassive black hole, converting gravitational energy to radiation. AGN have a wide range of observed properties: e.g. in their emission lines, radio emission, and variability. Most likely, these properties depend significantly on their orientation to our line-of-sight, and to unify AGN into physical classes it is crucial to observe their orientation-independent properties, such as the host galaxies. Furthermore, host galaxy studies are essential to understand the formation and co-evolution of galactic bulges and supermassive black holes. In this thesis, the main focus is on observationally characterizing AGN host galaxies using optical and near-infrared imaging and spectroscopy.

BL Lac objects are a class of AGN characterized by rapidly variable and polarized continuum emission across the electromagnetic spectrum, and core-dominated radio emission. The near-infrared properties of intermediate redshift BL Lac host galaxies are studied in Paper I. They are found to be large elliptical galaxies that are more luminous than their low redshift counterparts suggesting a strong luminosity evolution, and a contribution from a recent star formation episode. To analyze the stellar content of galaxies in more detail multicolor data, especially observations at blue wavelengths, are essential. In Paper III, optical - near-infrared colors and color gradients are derived for low redshift BL Lac host galaxies. They show bluer colors and steeper color gradients than inactive ellipticals which, most likely, are caused by a relatively young stellar population indicating a different evolutionary stage between AGN hosts and inactive ellipticals.

In Paper II, near-infrared imaging of intermediate redshift radio-quiet quasar hosts is used to study their luminosity evolution. The hosts are large elliptical galaxies, but they are systematically fainter than the hosts of radio-loud quasars at similar redshifts, suggesting a link between the luminosity of the host galaxies and the radio properties of AGN.

In Paper IV, the characteristics of near-infrared stellar absorption features of low redshift radio galaxies are compared with those of inactive early-type galaxies. The comparison suggests that early-type galaxies with AGN are in a different evolutionary stage than their inactive counterparts. Moreover, radio galaxies are found to contain stellar populations containing both old and intermediate age components.

CHAPTER 1

Introduction

This review gives a short background to infrared astronomy, Active Galactic Nuclei (AGN), and their host galaxies, for the general reader to understand the papers included in this thesis. Together with transient phenomena, such as gamma-ray bursts and supernovae, AGN are the most energetic known phenomena in the Universe, and they have been widely studied ever since their discovery in the 1960's (Schmidt 1963). AGN do not constitute just a single class of objects, but contain many subclasses covering a wide variety of activity levels from nearby Seyfert galaxies, with bolometric luminosities in the range of 10^{36} to 10^{38} W, to high redshift quasars, with bolometric luminosities up to 10^{42} W (c.f. bolometric luminosity of the whole Milky Way galaxy is $\sim 10^{37}$ W), with different kinds of observational properties at different wavelengths. Some AGN show very broad emission lines, while in some cases only narrow emission lines are seen. Also, AGN can be strong radio emitters, and may show very rapid variability and high polarization. Furthermore, observed properties depend on wavelength, and unlike in stars and inactive galaxies, the continuum emission from AGN is approximately constant over many orders of magnitude in frequency, indicating different physical emission processes for the radiation (e.g., non-thermal synchrotron radiation, bremsstrahlung, thermal blackbody). It is clear that the observed extraordinary properties cannot be explained only by stellar activity in the central region, but some kind of non-stellar energy production mechanism is inevitable. The currently accepted paradigm for the energy production in the central engine is the release of gravitational energy when gaseous material from the host galaxy falls toward the central supermassive black hole surrounded by a hot accretion disc and a molecular torus (Salpeter 1964, Lynden-Bell 1969). The efficiency of this process is far greater than that of thermonuclear fusion in stars.

Though AGN exhibit a wide range of observed properties, it does not necessarily imply that they are physically different. The unification model (e.g. Urry & Padovani 1995) has been developed to characterize their real physical appearance instead of their observed properties. The orientation of the object with respect to our line-of-sight may play a central role in the AGN classification. For instance, cool molecular material in a toroidal geometry surrounding the supermassive black hole can obscure the central region of AGN and, thus, only narrow emission lines originating farther away from the nucleus can be seen (Type 2 AGN). However, if the orientation of the object is such that the torus is not limiting the view to the nucleus, the very central region can be seen and broad emission lines appear in the spectrum (Type 1 AGN). To confirm the unification model of AGN, it is essential to observe orientation-independent properties, such as their host galaxies and large scale environments. However, AGN and star formation often co-exist, adding confusion to the above classification.

In the past decades, AGN have been widely studied in optical wavelengths, but

since the 1980's infrared technology has improved significantly and an ever increasing number of infrared observations have been carried out. In the host galaxy studies, especially, infrared observations are very useful due to low nuclear-to-host luminosity ratio and significantly reduced extinction. Also in studying the host galaxies, infrared has advantages over optical, because in optical wavelengths stellar features from a young population may be diluted by another emission component, such as the AGN continuum. Furthermore, the near-infrared contains many diagnostic stellar features that can be used as a stellar population indicator based on their dependence on stellar temperature and luminosity.

AGN offer a great platform to study exciting issues in modern astrophysics, such as black holes and intense gravitational fields. They give us an insight to the formation and co-evolution of galaxies and supermassive black holes. Furthermore, as very bright and distant objects (detected out to $z \sim 6$) they can be used as probes for mapping the intergalactic medium out to the huge distances.

The introductory review is organized as follows. Chapter 2 gives a short description of infrared astronomy, its observational techniques and its advantages in studying the stellar populations of quasar host galaxies. In Chapter 3 basic facts on the AGN classes, energy production mechanism and unified models are reviewed. Chapter 4 introduces the host galaxies of AGN and their evolution over cosmic time. Future directions of the work on the field of host galaxies are discussed in Chapter 5, and Chapter 6 presents the Papers themselves.

CHAPTER 2

Infrared astronomy

The human eye is sensitive to only a very narrow wavelength range, namely the visible window ranging from ~400 nm to ~700 nm. Our understanding of the Universe would be very limited and biased if our observations were based only on that narrow wavelength range. Fortunately, in the past few decades, significant technological improvements have expanded our observational capabilities both into longer and shorter wavelengths, including infrared radiation, allowing observations of celestial objects that otherwise would have been hidden from us, such as young star forming regions immersed in dust, luminous and ultraluminous infrared galaxies, the distant (high redshift) Universe, and the central regions of the Milky Way. This short introduction into the history and observational methods of infrared astronomy is by no means meant to be complete, but rather aims to give a concise insight into the field that is essential to understand the infrared observational data presented in the Papers.

2.1 Introduction

Nowadays, silicon based semiconductor CCD (Charge-Coupled Device) cameras have replaced photographic plates in astronomical observations. CCDs have been used in optical observations, covering the wavelength range from ~3000 Å to ~10,000 Å, since the 1970's. The most significant advantages of CCDs over photographic plates are their remarkably better quantum efficiency, ranging from 0.65 to 0.9 (Ando et al. 2004, Finger et al. 2004), and their linear response to incoming radiation. In semiconductor devices an incoming photon, with energy greater than the threshold energy of the semiconductor material, releases an electron from the valence belt and transfers it into the conducting belt. For materials used in optical detectors, the photon threshold energy is achieved at wavelength $\lambda = 1.05\ \mu$m, corresponding to energy E = 1.18 eV, and thus longer wavelength photons (i.e. infrared photons) do not have enough energy to transfer electrons into higher energy levels. For that reason, infrared detectors have to be made of semiconductor materials (e.g. HgCdTe, InSb, PtSi) with lower threshold energies than those in the optical.

Although infrared radiation was discovered a long time ago, infrared astronomy is still quite young due to difficulties in the detector technology. Because of their lower commercial interest, the technical properties of the materials used in infrared arrays are less well understood than the silicon-based materials in optical detectors, and thus they are less well developed. For these reasons, infrared detectors are not constructed as monolithic arrays like optical CCDs, but instead they are of hybrid construction, where an infrared-sensitive detector is bonded to a CCD-type readout array. This construction is, however, physically more fragile than a monolith

array, limiting the size of individual infrared arrays, and for instance differential thermal expansion may damage the array if it undergoes a large temperature change, e.g. from operational to room temperature. Furthermore, infrared arrays have larger read-out-noise than optical CCDs but in practice this is not a severe limitation, because the noise in infrared observations is typically dominated by the photon-noise from the high sky background.

Infrared astronomical technology has been available since the 1960's, and nowadays InSb and HgCdTe detectors are the most widely used detectors in the wavelength range of 1 – 5 μm. For these detectors, the energy gap between the valence and the conducting belts is lower (e.g. 0.23 eV for InSb) than those of silicon-based optical CCD detectors, and consequently they are suitable for observations in the infrared. First generation infrared arrays were very small containing only 60x60 pixels, and observations were limited by the small field-of-view (~20x20 arcsec). Current arrays are assembled from multiple individual detector cells containing millions of pixels (typically 2048x2048 pixels) with a large field-of-view (~4x4 arcmin), and are sensitive to infrared radiation over a large wavelength range from 1 to 300 μm. Note that some telescope facilities, e.g. *UKIRT* and *VISTA*, are nowadays equipped with near-infrared detectors that are capable of observing 0.2 – 0.5 square degree fields in a single exposure. To decrease the thermal noise, infrared detectors must be cooled to very low temperatures. For instance, InSb detectors are operated at ~30 K, while HgCdTe detectors can be used at slightly higher temperatures, ~60 – 80 K.

The infrared spectral region is divided into three main subregions, which are further divided into well-defined wavelength bands: near-infrared (1 to 5 μm) with *J-, H-, K-, L-* and *M*-bands, mid-infrared (5 to 30 μm) with *N*- and *Q*-bands (see Fig. 1), and far-infrared (30 to 370 μm). Infrared observations resemble those in the optical, but especially ground-based infrared observations are more complicated due to the influence of the Earth's atmosphere, for two reasons. First of all, most of the incoming infrared radiation is absorbed by atmospheric H_2O and CO_2 molecules, and thus observations are possible only in certain narrow wavelength bands. The transparency of the atmosphere in near- and mid-infrared is presented in Fig. 1. Secondly, the atmosphere itself radiates strongly at infrared wavelengths. In fact, this strong background sky emission causes the most significant difference between optical and infrared observations. In the near-infrared, the high background is mainly due to airglow OH-lines which are especially abundant in the *H*-band. Beyond 3 μm, the thermal black body radiation from Earth's atmosphere and the telescope itself begins to dominate the background. In mid-infrared, especially, the sky background is very strong and varies very rapidly, drastically limiting the integration time of a single exposure. To be able to subtract the sky background emission from the science frames, the position of the science object within the array must be varied slightly between each short single exposure. This technique is known as dithering. The sky background level is then represented by the median image combined from the dithered frames, which is then scaled and subtracted from each science frame. Alternatively, one can take separate sky frames, which are then subtracted from the science frames. In the mid-infrared, another technique, chopping, is also commonly used in which nearby regions of sky are observed by rapidly switching the secondary mirror between target and sky

positions, typically at frequency of a few Hz. The sky-corrected image is then obtained by subtracting the pair of images.

Near-infrared observations have several advantages over optical, because that wavelength domain traces much better the global mass-to-light ratio of galaxies, it is much less contaminated by very recent star formation and scattered AGN light, and extinction is significantly reduced. Moreover, one major advantage in host galaxy studies is that the nuclear-to-host luminosity ratio is minimized in the near-infrared, thus allowing for accurate AGN/host galaxy decomposition to be obtained.

Ground-based infrared observatories are preferentially located at high-altitude and dry places (e.g. Hawaii, Chile), to minimize the path length in the atmosphere, and thus to have a smaller amount of H_2O and CO_2 absorption. However, no matter how high or dry place the observatory is located in, the atmosphere will remain transparent only in certain narrow wavelength ranges. Thus, to be able to perform observations over the whole wavelength range from near- to far-infrared, telescopes must be launched above the atmosphere (see Section 2.4.).

2.2 History

Infrared radiation was discovered in 1800 with a calorimetric experiment by William Herschel, who directed sunlight through a glass prism and measured the temperature of each color of the spectrum. This measurement indicated that some previously unknown invisible radiation beyond the red end of the spectrum contained more heat than the visible colors. It was soon demonstrated that these "calorific rays" had similar reflection, absorption, and transmission properties to visible radiation. This simple experiment showed that visible wavelengths are in fact only a small part of the whole electromagnetic spectrum. The next major step forward in infrared observations was taken in 1878 when Samuel Langley developed the first infrared bolometer, which was subsequently used to study infrared radiation from the Sun. However, the first systematic observations of celestial objects had to wait until 1920 when, e.g.. S. B. Nicholson and E. Pettit used a vacuum thermocouple to study infrared radiation from the Moon, planets and bright stars, including the first measurements of the diameter of giant stars.

A major advancement in infrared astronomy technology came in the early 1950's when the first lead-sulfide (PbS) detectors were developed, allowing observations up to 3 μm. However, to increase their sensitivity, these detectors were restricted to be used only at low temperatures (77 K). The next breakthrough in sensitivity was achieved in 1961 when PbS was replaced by germanium (Ge) as the detector material of choice for bolometers. The usefulness of Ge arises from the fact that it changes its conductivity corresponding to incoming infrared radiation. Furthermore, Ge-based detectors were also suitable for far-infrared observations.

With improving detector technology, infrared observations expanded to longer and longer wavelengths and to measure emission meaningfully, it became necessary to define a reference system based on infrared photometric magnitudes. The near-infrared

magnitude system still in use today (*JHKLM*-bands) was derived by Johnson (1966) dividing the infrared region into several narrow well determined wavelength bands where the atmosphere is transparent, covering wavelengths up to 4 μm. Similar photometric bands were later defined also in the mid-infrared (*NQ*-bands).

2.3 Extinction

One of the advantages of infrared observations, together with an optimal nuclear-host luminosity ratio and the capability of tracing stellar population, is the remarkably lower extinction than in the optical. Extinction is caused by small solid interstellar dust grains with sizes ranging from a few wavelengths of light to the size of large molecules. The level of extinction depends on the chemical composition and geometry of the dust grains, and the wavelength of incoming radiation. There are two main processes contributing to extinction: absorption and scattering. In absorption, the incoming photon is absorbed by a dust grain and re-emitted in the infrared. On the other hand, in scattering the incoming photon is scattered by a dust grain, but the intrinsic wavelength of the photon is unchanged. Scattering dominates extinction in the optical and near-infrared, whereas it is insignificant compared to absorption in mid- and far-infrared (Weingartner & Draine 2001).

Extinction varies with wavelength, being strongest for short wavelength radiation. The detailed shape of the extinction curve depends on the exact composition of the interstellar medium which varies from galaxy to galaxy. The extinction curve is best known for the Milky Way, Large Magellanic Cloud (LMC) and Small Magellanic Cloud (SMC), presented in Fig. 2. Their extinction curves show a prominent feature, so-called ultraviolet bump, at 2175 Å (e.g. Cardelli et al. 1989). The cause for the bump is still unknown. In the infrared, there are several extinction features related to silicate materials, e.g. the absorption features at 9.7 and 18 μm.

Because of the strong wavelength dependence, extinction is significantly reduced in the infrared. For instance, extinction in the near-infrared *K*-band ($\lambda = 2.2$ μm) is only 1/10 of that in the optical *V*-band. The central regions of a large number of galaxies, including the Milky Way, show very high extinction, and they are completely obscured in the optical wavelengths. Similarly, e.g. young star forming regions are usually completely hidden by dust in the optical, but show bright emission in the infrared. Extinction can most readily be derived by using hydrogen emission line ratios, such as optical Balmer lines (usually Hα/Hβ) and near-infrared Paschen and Brackett lines, with some assumptions about intrinsic conditions. If there are no suitable emission line pairs available for extinction measurements, continuum colors can also be used, provided that the intrinsic (unobscured) colors of the class of objects are known.

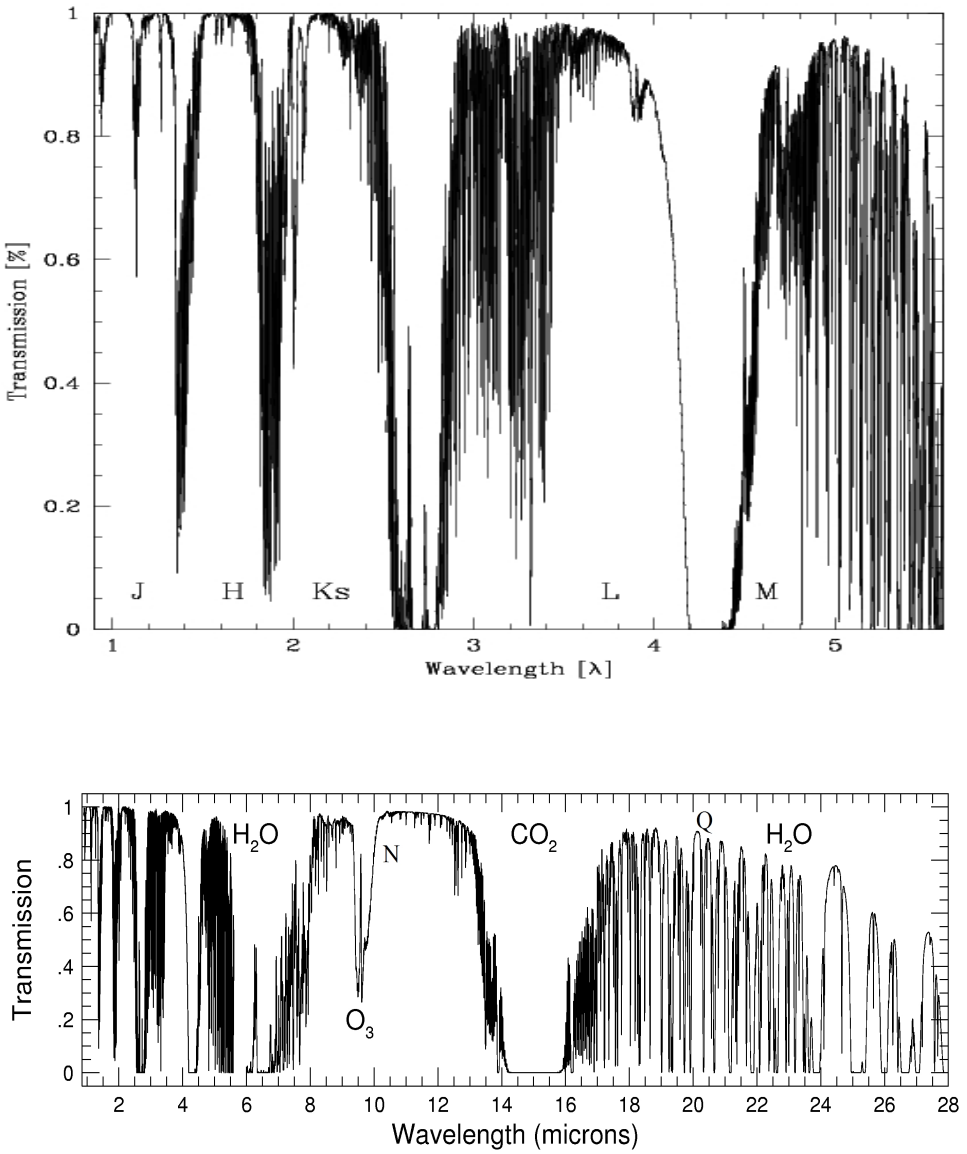

Figure 1: The transparency of the atmosphere at near-infrared (JHKsLM bands; upper panel) and mid-infrared (NQ bands; lower panel) wavelengths, together with the most prominent absorption components. (Gemini Observatory)

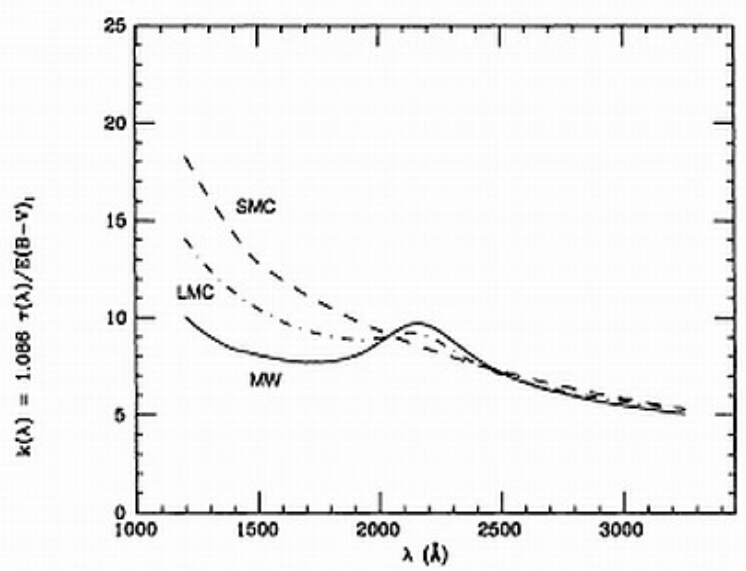

Figure 2: The variation of extinction as a function of wavelength for Milky Way, LMC and SMC. The most prominent feature, the ultraviolet bump of MW and LMC, is evident at 2175 Å (Calzetti et al. 1994).

2.4 Infrared observations from space

As was already stated, ground-based infrared observations are significantly restricted by the atmospheric thermal background emission, and the transparency of the atmosphere in only narrow wavelength bands. To avoid those problems, infrared detectors need to be launched above the atmosphere. The first high altitude airborne infrared detectors were set up with balloons and rockets in the 1960's. In 1966 balloons were used to observe 120 bright infrared sources in the plane of the Milky Way at 120 μm by the Goddard Institute of Space Science. However, balloon based observations are strongly restricted by their short observing time. Rocket technology developed rapidly in the 1960's and it was also applied to infrared observations. Like balloons, rockets can be used only for a very short time for a single observation. Despite these restrictions, the first infrared all-sky map was produced from several flights by the Air Force Cambridge Research Laboratory. It covered ~90% of the sky at wavelengths 4.2, 11, 20 and 27.4 μm, and detected over 2000 infrared sources. High altitude converted airplanes have also been used to carry infrared detectors, such as the long-standing *KAO* (Kuiper Airborne Observatory; e.g. Dunham 1995). In fact, airplanes are still a viable option for infrared observations, as testified by e.g. *SOFIA* (Stratospheric Observatory For Infrared Astronomy) which will be an optical-infrared-submillimeter telescope, planned to be operational from 2009 (e.g. Becklin et al. 2007).

Satellites are preferred over balloons and rockets for infrared observations because, in Earth's orbit, they are above the disturbing atmosphere and are capable of observing the whole range of infrared wavelengths without limitations on their observation time. The first infrared satellite, the 60 cm *IRAS* (Infrared Astronomical Satellite) was launched in 1983 and was operational for 10 months (Neugebauer et al. 1984). It did not have high resolution imaging capabilities, but provided the first high sensitivity all-sky survey at 12, 25, 60 and 100 μm detecting over half a million infrared sources, doubling the number of then known infrared emitters. *IRAS* detected, for instance, a new class of (ultra)luminous (often interacting) infrared galaxies, whose bolometric radiation is dominated by infrared emission (Soifer et al. 1986, 1987). Furthermore, while inactive galaxies contain cold dust with temperature T ~ 30 K, *IRAS* revealed that in infrared galaxies the temperature of dust is considerably higher, T = 100 – 300 K (de Grijp 1992).

IRAS was followed by the Japanese *IRTS* (Infrared Telescope in Space; e.g. Murakami et al. 1996) and the European 60 cm *ISO* (Infrared Space Observatory; e.g. Cesarsky & Salama 2006) telescopes in 1995. *ISO* was operational for four years, and it was capable of observations between 2.5 and 240 μm, and achieved significantly higher sensitivity and higher spatial resolution than *IRAS*. Importantly, *ISO* was the first space telescope with spectroscopic capability.

The latest, currently operational, infrared satellite, *Spitzer*, launched by NASA in 2003, consists of a 0.85 m diameter telescope and is capable of observing in the wavelength range of 3 – 180 μm at higher sensitivity and spatial resolution than any previous space observatory (e.g. Werner et al. 2004). The next European infrared-submillimeter satellites, the 3.5 m diameter *Herschel Space Observator*y and the *Planck Surveyor*, will be launched in 2009. Herschel can be used for imaging and spectroscopic observations from 60 to 670 μm, while Planck will perform all-sky mapping of anisotropies of the cosmic background radiation. Finally, it is worth to note that the *HST* (Hubble Space Telescope) has the *NICMOS* (Near Infra-Red Camera and Multi-Object Spectrometer) detector since 1997, which is capable of imaging and spectroscopy observations in the wavelength range of 0.8 – 2.5 μm.

2.5 Sources of infrared emission

All objects with temperature above absolute zeropoint emit electromagnetic radiation, and the wavelength at which this blackbody radiation is most intense depends on the temperature of the object according to Wien's law. The average spectral energy distribution (SED) of a radio-quiet quasar, starburst galaxy, LINER, and inactive spiral galaxy are presented in Fig. 3. Note that the continuum emission from a quasar is approximately constant over a wide frequency range. Infrared wavelengths correspond to temperatures of a few hundred Kelvins (e.g., room temperature of T = 300 K corresponds to mid-infrared $\lambda = 10$ μm). Two main sources dominate the infrared emission of a typical galaxy: Cool M-type giant and supergiant stars in the near-infrared, and thermal emission from warm or cold dust at longer wavelengths.

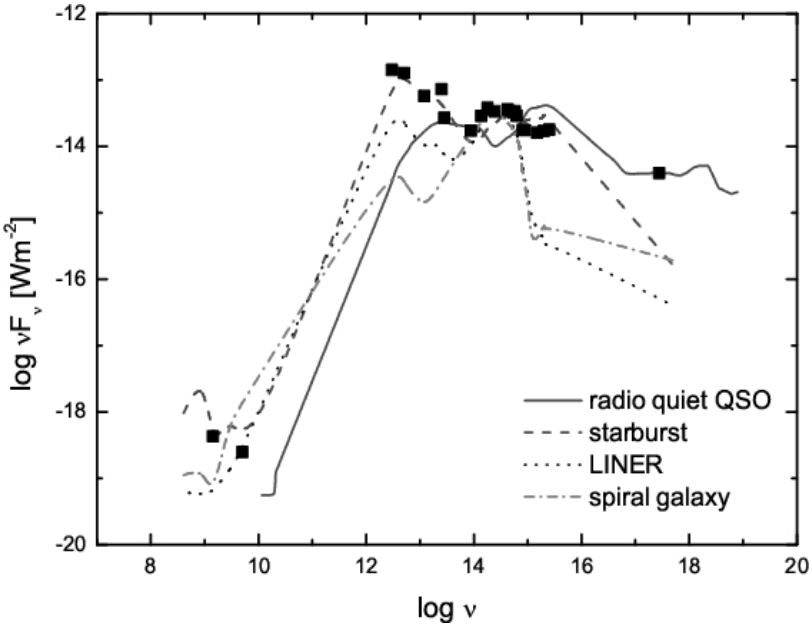

Figure 3: The average spectral energy distribution of a radio-quiet quasar compared with that of a starburst galaxy, a LINER and an inactive galaxy (Zuther et al. 2007).

Dust cannot survive very high temperatures before sublimation beyond T ~ 1000 K. Thus, direct thermal emission from dust is not significant at the near-infrared regime, but its contribution increases rapidly at $\lambda > 2.5\ \mu$m and becomes dominant over the stellar component at mid- and far-infrared. For instance, the mid-infrared emission from zodiacal light is due to dust in the plane of the Solar system. In the far-infrared, radiation is dominated by emission from cold giant molecular clouds (T < 150 K). These clouds are associated with star forming regions and contain dust with high densities and low temperatures (Schulz et al. 2007, Arnal et al. 2008), corresponding to blackbody radiation at mid- and far-infrared at $\lambda > 30\ \mu$m. Because these star forming regions are buried inside high density clouds with very high optical extinction, infrared observations are paramount to obtain information about the earliest stages of star formation.

In addition to continuum emission from stars and dust, the infrared spectral region is full of diagnostic absorption and emission lines. Absorption features originate mostly in stellar atmospheres due to a number of atomic and molecular components, such as hydrogen recombination lines, CaI, and molecular CO. The strength of the absorption features increases with stellar metallicity. However, this relation is non-linear and synthetic stellar models are needed to predict the absorption line strengths (e.g., Fioc & Rocca-Volmerange 1997, Bruzual & Charlot 2003, Maraston 2005). Infrared absorption features are especially useful in studying the unresolved stellar

populations of galaxies, as will be further discussed in the next Section.

While stars dominate the absorption lines in the integrated spectra of galaxies, stellar spectra contain only a few emission lines (e.g. H and He lines from hot stars), while the majority of infrared emission lines arise from interstellar nebular gas. They can be divided into three main categories according to the temperature of the gas: Molecular lines, (e.g. H_2) with temperature $T < 2000$ K, atomic lines (e.g. HI) with temperature $T \sim 10^4$ K, and highly ionized coronal lines (e.g. [SiVII]) with temperature $T \sim 10^5$ K.

2.6 Absorption lines as stellar population indicators

The stars that dominate the near-infrared emission of galaxies are significantly different from the major population in the visible wavelengths. In the near-infrared, the largest contribution to the luminosity of a typical galaxy comes from cool M- and K-type giant and supergiant stars, whereas a much wider range of stellar types contributes to radiation in optical wavelengths. Thus, prominent near-infrared stellar absorption features can be used as indicators for the stellar population in composite stellar systems which is based on their dependence on stellar temperature and/or luminosity (Kleinmann & Hall 1986, Ali et al. 1995, Ramirez et al. 1997). Furthermore, due to the much lower extinction, near-infrared is preferential over optical for studying dusty nearby galaxies (e.g. Mannucci et al. 2001).

The most widely studied near-infrared absorption features are atomic SiI (1.589 μm), and molecular CO(6-3)(1.619 μm) in the *H*-band, and atomic NaI (2.207 μm) and CaI (2.263 μm) and molecular CO(2-0) bandhead (>2.29 μm) in the *K*-band. Temperature sensitivity can be used to divide stars to different spectral types, e.g. strength of CO(6-3) feature increases from early-K to late-M stars (i.e. with decreasing temperature), while SiI is only weakly dependent on temperature. However, especially the *H*-band is very rich in absorption features, and there are contributions to each line by more than one absorption component. For instance, especially in cool stars, the CO(6-3) feature is slightly contaminated by OH-lines but, however, its contribution is always less than 30% in stars with temperature $T < 3000$ K (Origlia et al. 1993). Similarly, SiI dominates the 1.589 μm feature at temperatures $T_{eff} > 3500$ K. The most useful diagnostic line pattern is the *K*-band ^{12}CO first overtone, the depth of which is predicted to be sensitive to stellar population parameters (e.g. Vazquez et al. 2003). The CO bandhead is very strong in young giants and supergiants, and strong in cool AGB stars, while it becomes weaker in older population. The variation of the strength of the CO(2-0) bandhead in giant and main sequence stars, from spectral type G to M, is presented in Fig. 4. Because the CO(6-3) and SiI features are very close in wavelength, together with the CO(2-0) bandhead, they can also be used to estimate the contribution of dilution from a non-stellar continuum emission source, e.g. an AGN, in both *H*- and *K*-bands by plotting the line ratios CO(1.62)/SiI(1.59) and CO(1.62)/CO(2.29) against the strength of the CO(1.62) feature (e.g. Oliva et al. 1995).

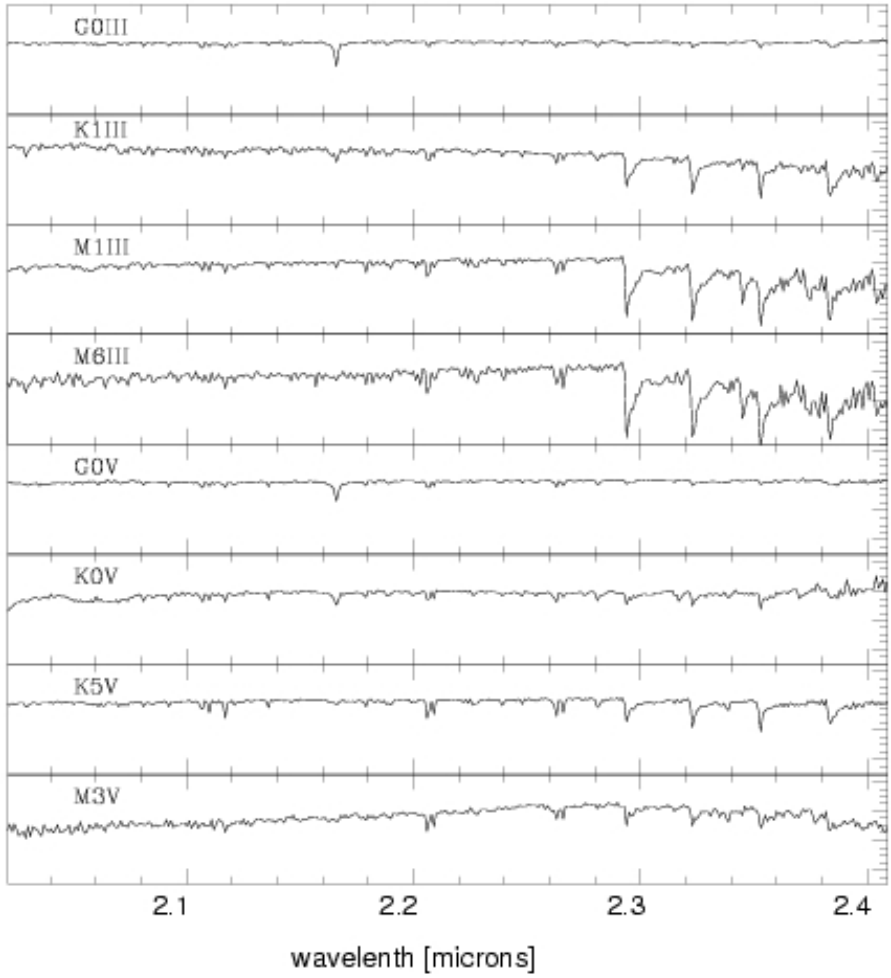

Figure 4: The strength of the CO(2-0) bandhead ($\lambda > 2.29\,\mu m$) and the Br-γ absorption feature at $\lambda = 2.166\,\mu m$ in giant (III) and main sequence (V) stars. Spectra adapted from Wallace & Hinkle (1996).

Currently, there are no self-consistent spectral synthesis models for the theoretical derivation of near-infrared spectra for composite stellar systems. Instead, one has to rely on the comparison of observed spectra with near-infrared stellar atlases (e.g. Lancon & Rocca-Volmerange 1992, Wallace & Hinkle 1996).

CHAPTER 3

Active galactic nuclei

Active Galactic Nuclei (AGN) have been studied extensively for the past four decades. The field of AGN studies is very extensive, containing research from the physics of nuclear supermassive black holes to their large scale environments, and thus it is an overwhelming task to describe all the AGN types completely here. The main focus of this Chapter is to give the reader an overall picture of the AGN phenomenon, its energy production mechanism and the unification model.

3.1 Introduction

Galaxies are the building blocks of the Universe, forming structures all the way from small galaxy groups (like our Local Group) with a few dozen members, to large galaxy clusters (like the Virgo cluster) containing thousands of galaxies. The initial seeds of galaxies were formed in the very early Universe, the relic of which can still be observed in the form of the cosmic microwave background radiation. However, the growth and evolution of these seeds from the distant past to the present epoch is not completely known yet.

Based on their morphological classification, the majority of nearby galaxies are either spiral or elliptical galaxies. At first sight, they appear to show no clear differences from object to object, but when analyzed in more detail, some of them turn out to have peculiar properties, such as exceptionally bright star-like nuclei and unusual emission lines (e.g. Slipher 1917). Studying such spiral galaxies in 1943, Carl Seyfert found that, unlike most spirals, the galaxies in his sample showed unusually broad or atypically highly ionized permitted and forbidden emission lines in their nuclear spectrum (Seyfert 1943). These objects became known as Seyfert galaxies, and they were the first galaxies that were found to exhibit enhanced activity in their central regions, i.e. the first discovered type of AGN.

However, that was just the beginning! During the 1960's it was found that the spectrum of a bright star-like object, associated with the radio source 3C 273, deviated strongly from typical stellar spectra, in that the spectrum of 3C 273 was dominated by emission lines. These lines, however, could not be identified with any known elements. Eventually, this spectacular object was explained by postulating that it actually resides at a cosmological distance ($z = 0.16$) and that the (mostly hydrogen) emission lines were redshifted to unfamiliar locations in the spectrum (Schmidt 1963). Soon after, Greenstein & Schmidt (1964) showed that another radio source, 3C 48, was a similar type of object, at an even higher redshift of $z = 0.37$. Subsequently, through sky surveys, more and more similar objects at higher and higher redshifts were identified. On photographic plates they only showed up as point-like objects, and this class of

AGN became known as quasi-stellar radio sources, or quasars for short. For a more detailed discussion of the history of the discovery of AGN, see e.g. Shields (1999).

Quasars were at first mainly found by their radio emission, and thus the majority of the first identified quasars were strong radio emitters. For the definition of radio-loudness, either R parameter or radio luminosity at 5 GHz is used. The R parameter defines the ratio between radio and optical fluxes, and the ratio of $R = 10$ is adopted for the boundary value between radio-loud and radio-quiet objects. Radio-loud AGN have $R \sim 1000$, whereas radio-quiet AGN have $R \sim 1$ (Strittmatter et al. 1980, Kellermann et al. 1989). Alternatively, radio luminosity at 5 GHz is used as a definition for radio-loudness such that AGN with luminosities higher than $2.5 \times 10^{24} h_{100}^{-2}$ W Hz^{-1} are classified as radio-loud.

The domination of radio-loud objects changed dramatically when surveys at other wavelengths were carried out, and e.g. only ~10% of all the currently known optically selected quasars are radio-loud (Kellermann et al. 1989). Nowadays, regardless of the properties of their radio emission, these objects are called quasars. As will be discussed in Section 3.4, a large variety of objects with a huge range in the level of their nuclear activity have been found ever since, e.g. LINERs (Low Ionization Nuclear Emission line Region), giant elliptical radio galaxies with extended radio emission lobes, and rapidly variable blazars. Irrespective of the morphological type of their host galaxy, all the objects that show evidence for nuclear activity, are grouped into a common class of AGN. This veritable AGN zoo has been studied for more than 40 years now, and their research remains a very active and leading field in astronomy.

3.2 AGN surveys

Because AGN candidates appear as point sources in imaging surveys, they have to be separated from ordinary stars. Unfortunately, their identification is not a straightforward task, because only nearby AGN are resolved in the sense that they can be easily associated with an underlying galaxy, while the majority of AGN, such as quasars, are only seen as point-like objects. Their identification can be obtained by using properties that are characteristic for AGN, such as variability, ultraviolet excess (UVX), and infrared, radio, and X-ray emission.

AGN have typically broad continuum emission over a large wavelength range with ultraviolet excess, deviating strongly from main sequence stars. The $U - B$ color for the hottest main sequence stars is typically $U - B \sim 0.4$, whereas for AGN it is significantly bluer, $U - B \sim -0.8$, assuming a power law $F(\nu) \propto \nu^{-\alpha}$ with spectral index $0.5 < \alpha < 1$. This spectral difference can be taken advantage of in AGN identification by imaging the objects in at least two different filters, such as in the U- and B-bands (e.g. Markarian 1967, Markarian et al. 1981, Boyle et al. 1990). These UVX surveys exclude most of the main sequence stars, but can still be contaminated by white dwarfs. Thus, each AGN candidate has to be verified through (time consuming) spectroscopy. The UVX method is not failsafe. Firstly, it is limited to redshifts $z < 2.2$ because at higher redshifts characteristic AGN emission lines are redshifted from the

U-band into the *B*-band, hence reddening the $U - B$ color. Secondly, two broad band colors cover only a relatively narrow wavelength range and, thus, a large number of objects with different spectral types may remain unidentified.

To avoid problems encountered in surveys carried out only in two filters, AGN surveys have also been performed in multiple filters, typically *U, B, V, R, I* (e.g., Warren et al. 1991, Kennefick et al. 1995). Contamination due to white dwarfs is avoided by using multiple filters because, while the spectra of white dwarfs and AGN are similar in a narrow wavelength range, they have different intrinsic spectral shapes over a wide wavelength range. Furthermore, multicolor surveys are not limited to blue objects but can also be used to find red AGN. One major difficulty remains in all color surveys, namely the absorption of radiation by interstellar/intergalactic dust and gas, which makes distant objects too faint to be observable. To avoid the absorption problem in highly obscured objects, infrared observations can be used to search for AGN, because they have enhanced flux at the mid-infrared spectral domain. The first comprehensive four-color (12, 25, 60 and 100 μm) all-sky infrared survey was carried out by *IRAS* satellite, although it was limited by rather low angular resolution. However, infrared surveys lack the unambiguity of e.g. X-ray surveys, because some inactive galaxies also radiate strongly in infrared.

Unlike stars, the majority of AGN show strong optical and UV emission lines in their spectra, providing another efficient way to find AGN. They are especially useful to identify high redshift AGN and provide a complementary method for UVX surveys. AGN spectral lines are strong, therefore low dispersion spectra are sufficient for identification of AGN candidates. Higher dispersion spectra are then required to confirm their AGN character and redshift. Slitless spectroscopic surveys have been carried out in the past decades, e.g. the Large Bright Quasar Survey produced a large sample of quasars (~ 1000) with magnitude $16 \leq z \leq 18.5$ in redshift range $0.2 < z < 3.4$ (Hewett et al. 1995).

Although only minority of AGN are radio-loud, radio observations are also suitable to survey AGN, especially high redshift objects that have not been found by UVX surveys. An advantage of radio observations is that the position of a target can be determined to subarcsec accuracy. Thus, there is usually only one optical counterpart in the error box of the AGN candidate. Because of the power law spectrum of radio sources, flat spectrum AGN (with spectral index $\alpha > 0.5$) dominate high frequency (~ GHz) surveys. Several radio surveys have been carried out, e.g. by the Parkes Radio Observatory to observe the southern sky at 2.7 GHz (Wall et al. 1976), and by the *NRAO* to survey the northern sky at 1.4 and 5 GHz (Pauliny-Toth & Kellermann 1972). More recently, the *FIRST* survey, carried out by VLA, surveyed the northern radio sky at 20 cm with a 5 arcsec resolution (e.g. Becker et al. 1995, Gregg et al. 1996).

Unlike ordinary stars and inactive galaxies, AGN emit X-rays, providing another suitable way for their detection. In the past decades, a few X-ray surveys have been carried out, *HEAO-1* All-sky survey (Piccinotti et al. 1982), *EINSTEIN EMSS* (e.g. Gioia et al. 1990), and *ROSAT* deep survey (Boyle et al. 1993). EMSS is a complete flux-limited survey of 835 sources, and has 95 % complete optical identifications (Stocke et al. 1991). *ROSAT* all-sky survey observed more than 60000 sources in 0.1 – 2 keV soft X-rays.

Two major recent AGN surveys are the 2dF survey, based on the UVX method of photographic plate material (Croom et al. 2004), and the SDSS (Sloan Digital Sky Survey), which uses multicolor imaging to separate AGN candidates from stars (Fan 1999, Richards et al. 2001).

3.3 The structure and energetics of AGN

As was stated in Chapter 1, together with transient phenomena, such as gamma-ray bursts and supernovae, AGN are among the most energetic objects in the Universe. According to the current paradigm, a supermassive black hole (SMBH) lies in the center of all AGN, surrounded by an accretion disc. Further away, in the Broad Line Region (BLR), gas clouds are orbiting the central region, and are emitting observable broad emission lines in the spectrum. This central structure is surrounded at larger distances by a partly obscuring molecular torus, and narrow emission line gas clouds in the Narrow Line Region (NLR). This schematic, somewhat simplified model of the structure of the AGN is presented in Fig. 5.

Observational evidence for supermassive black holes

The most crucial factor in the current AGN paradigm is the existence of SMBHs, because even the most convincing theory remains only a hypothesis without supporting observational evidence. While, naturally, a black hole itself does not emit any observable radiation, its presence can be inferred from dynamical measurements of the bulk motion of gas and stars orbiting the black hole. As is discussed below, the observational evidence for the existence of SMBHs is overwhelming, supporting the only model that is capable of explaining even the most luminous AGN and their radio emission properties.

One of the earliest such observations is of an SMBH in the nearby giant elliptical galaxy M87 in the Virgo cluster. The existence of the SMBH was confirmed by spectroscopic studies of the dynamics of stars in the central region with the *HST* (e.g. Ford et al. 1994, Harms et al. 1994). Furthermore, recent observations are also consistent with a spinning SMBH in the center of M87 (Wang et al. 2008). However, perhaps the strongest evidence for the presence of an SMBH in AGN comes from radio VLBI interferometric H_2O megamaser observations of the nuclear region of NGC 4258 (Miyoshi et al. 1995). Assuming that the masers are orbiting the nuclear region in near-Keplerian orbits, the blue- and redshifted velocity measurements of the masers allow one to calculate the enclosed mass within the central 0.13 pc radius of NGC 4258. This mass, 3.6×10^7 $M_\odot$, can only be explained by a SMBH. Dynamical measurements have since revealed rapid rotation and large velocity dispersions, indicative of similar mass concentrations, in the centers of many other galaxies including the Andromeda and the Milky Way (Kormendy 1988, Ghez et al. 2000, Schödel et al. 2002, 2007). Especially, the velocities of stars in a cluster orbiting the nucleus of our own Galaxy,

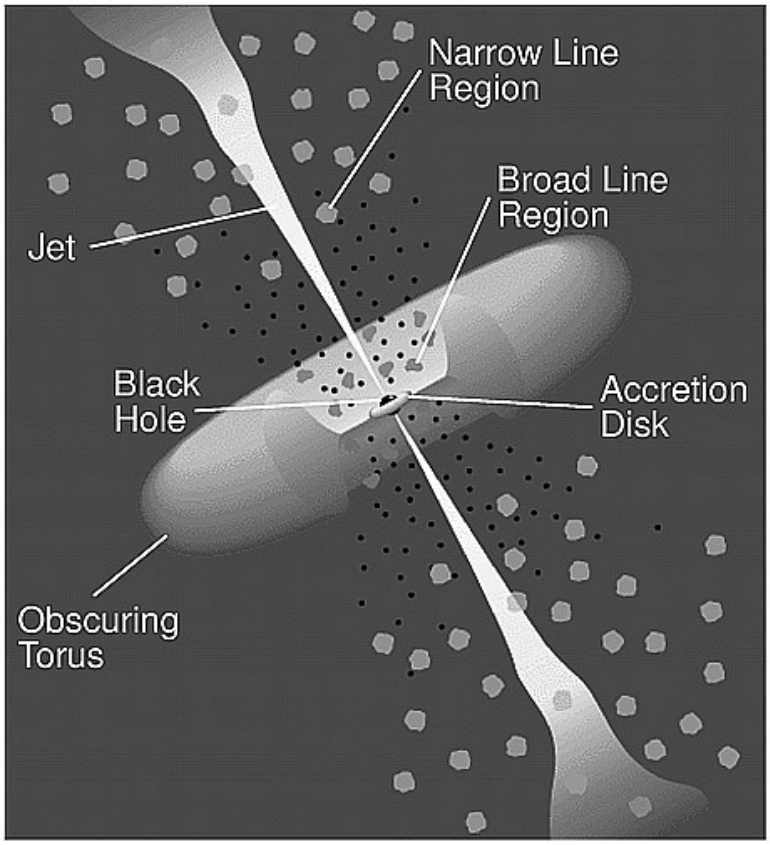

Figure 5: A schematic cutaway view of the structure of radio-loud AGN. A typical radius of the obscuring torus is a few tens of parsecs. The sizes of the components are not to scale. (Urry & Padovani 1995)

Sagittarius A* (Balick & Brown 1974, Eckart & Genzel 1997), have been observed for a long period of time in order to derive their orbits around the central mass concentration. The near-Keplerian orbits of such stars within the radius of $r = 0.02$ pc indicates the presence of a mass of 3×10^6 $M_\odot$ in the center of the Milky Way.

Energy production of AGN

AGN are observable across vast distances, and therefore it is obvious that they must be intrinsically very luminous objects. The energy output of AGN can be as large as $L \sim 10^{14}\ L_\odot$, significantly greater than those of inactive galaxies (for instance, the luminosity of Milky Way is $L \sim 10^{11}\ L_\odot$). Naturally, this raises the fundamental question of how is that energy generated? In the early days of AGN studies, a wide range of

candidates were suggested, such as gravitational and thermonuclear energy extraction from supermassive stellar clusters (Hoyle & Fowler 1963). This idea was later revived in the form of the nuclear starburst model (e.g. Terlevich et al. 1992), where the energy for the ionized clouds comes from a nuclear cluster of young massive stars and subsequent supernova explosions that form a fast moving shock front sweeping up surrounding material. Kinetic energy of the shock front is converted to radiation in the BLR. However, this occurs on very short timescales and most of the energy is radiated after only a few years. The essential parameter for the model is the rate of supernova explosions to maintain the luminosity over a reasonably long time. While starbursts are viable to, in principle, produce the observed energy and play an important role in the low luminosity AGN, e.g. in LINERs (Ho et al. 2001), they can not explain all the observed phenomena in AGN, such as their powerful relativistic collimated radio jet emission, or the powerful X-ray emission and rapid X-ray variability (e.g. Green et al. 1993, Kukula et al. 1998). In addition, the nuclear star cluster would have to be very compact, since even the nearest AGN, NGC 4395, remains unresolved with *HST* (Filippenko & Ho 2003).

Nowadays, the most prominent and widely accepted paradigm for the energy production mechanism is the transformation of gravitational potential energy into radiation due to viscous dissipation in a rotating accretion disc surrounding a central SMBH (Lynden-Bell 1969, Rees 1984). This is supported by recent observations which have shown that the most (or even all) of the nearby inactive spheroids contain a SMBH in their center (Ferrarese 2002, Barth et al. 2004, Combes 2005, Ferrarese 2006). The nuclear activity occurs in a physically very small region, and it can be understood in terms of gas falling toward the SMBH. For a non-rotating BH the size of the energy production region can be approximated by the Schwarchild radius $R_S = 2GM_{BH}/c^2$, where M_{BH} is the mass of the BH. For instance, for a BH of 10^8 solar masses, the Schwarchild radius is $R_S \sim 2$ AU. Thus the energy output is concentrated into a very compact region, being consistent with the rapid variability of AGN, characteristic especially to blazars.

A rotating (Kerr) BH within an external magnetic field offers a very efficient energy extraction mechanism (Wilson & Colbert 1995). According to the theory of general relativity, the extracted energy can be as high as tens of per cents of the rest mass of the gas. For comparison, the efficiency of nuclear fusion in stellar interiors is only ~0.7% of the rest mass. The total power radiated by a rotating BH can be approximated by the following equation (Blandford & Znajek 1977, Thorne et al. 1986),

$$P \sim 10^{20} \left(\frac{M_{BH}}{M_{sun}} \right)^2 \left(\frac{B}{1\mathrm{G}} \right)^2 \left(\frac{J}{J_{max}} \right)^2$$

given in [ergs^{-1}], where M_{BH} is the mass of the central BH, B is the strength of the external magnetic field, and J and J_{max} are the angular momentum and the maximum possible angular momentum, respectively. Assuming reasonable values, $M_{BH} = 10^8\,M_\odot$ and $B = 10^4$ G, the extracted energy from the SMBH is $P \sim 10^{44}$ ergs^{-1}, which is sufficient to produce the observed luminosity for most quasars. However, it is

approximately two orders of magnitude smaller than the Eddington luminosity $L_{\rm Edd}$ with a similar black hole mass. Increasing the black hole mass by the order of magnitude, output energy is sufficient for the energy production of nearly all AGN. Note that the vicinity of the central region is very complex, including electric and magnetic fields, shock waves and high energy particles, which all simultaneously reside within a region with a very small angular size.

The BH itself is, by definition, totally black, i.e. it does not radiate outwards, but its near environment does strongly so. Particles with mass and angular momentum do not fall directly into the BH, but they settle into an orbit around the nucleus. To continue their infall, these particles have to lose their angular momentum. Indeed, the observed radiation does not originate from the BH itself, but from the surrounding accretion disc, where the particles collect. Decreasing angular momentum at the inner edge of the disc is compensated by increasing the outskirt radius, but it can also be coupled to some external medium, such as a magnetic field. Actually, it is argued that such fields may also play a crucial role in the formation of the collimated jets of AGN (e.g. Li et al. 1992, Fendt 1997, Keppens et al. 2008).

The accretion disc surrounding a BH rotates differentially, and due to viscous interactions between gas particles, a temperature gradient is formed. The inner edge of the disc is heated to very high temperatures, radiating at UV wavelengths, while the cooler outskirt emits at longer, optical wavelengths. AGN X-ray emission is widely though to be due to inverse compton scattering from very high energy electrons residing in a corona above the accretion disc. The temperature of gas at the last stable orbit ($3R_{\rm S}$ for a non-rotating, and $1.5R_{\rm S}$ for a rotating BH) can be as high as $T \sim 10^5$ K and, indeed, the overwhelming luminosity of AGN is due to the emission from the accretion disc (except in the case of blazars, whose radiation is dominated by a relativistic jet).

The luminosity of the AGN produced by the accretion mechanism can be estimated by

$$L = \eta \dot{M}_{ac} c^2$$

where $\dot{M}_{ac}$ is the mass accretion rate, and η is the efficiency of the conversion process of mass to energy. Typically, the conversion factor $\eta \sim 0.1$, but it depends on the rotation of the black hole, varying from ~0.05 to ~0.3 for non-rotating and maximally rotating black hole, respectively. Typical accretion rates needed to produce the observed luminosity of AGN are rather low, only of the order of a few $M_\odot\,{\rm yr}^{-1}$. However, the luminosity radiated by spherically symmetric accretion onto a BH can not increase beyond a natural limit, called the Eddington luminosity, given by

$$L_{Edd} = \frac{4\pi G M_{BH} m_p}{\sigma_T} = 1.3 \times 10^{38} \frac{M_{BH}}{M_{sun}}$$

in [ergs^{-1}], where G is the gravitational constant, $M_{\rm BH}$ is the mass of the SMBH, $m_{\rm p}$ is the mass of a proton, and $\sigma_{\rm T}$ is the Thomson cross section. Above this luminosity, the

outward force of radiation pressure becomes larger than the inward force of gravity, stopping the accretion. The luminosity decreases, decreasing the radiation pressure, allowing accretion to start again.

A timescale for the growth of the central black hole mass can be approximated by combining the equation of the Eddington luminosity with the equation of the mass accretion luminosity. Thus the differential equation of the timescale is given as

$$\frac{dM}{dt} = \frac{L}{(\eta c^2)} = \frac{1}{\tau} M$$

where τ is given in years

$$\tau = \frac{L_{Edd}}{L} \frac{c \eta \sigma_T}{4 \pi G m_p} \simeq 4 \times 10^8 \eta \frac{L_{Edd}}{L}$$

The differential equation can be integrated to give

$$M(t) = M_0 \mathrm{e}^{t/\tau}$$

showing that the growth of a black hole occurs exponentially. Assuming a black hole is accreting at the Eddington limit, a timescale to build a 10^9 $M_\odot$ supermassive black hole is $t_{AGN} \sim 10^9$ years.

Emission line regions and the molecular torus

Gas clouds in the BLR, residing between the accretion disc and the molecular torus, are characterized by the broad wings to their spectral lines, associated with velocities up to 35000 kms^{-1} (see e.g. review by Sulentic et al. 2000). The non-homogeneous clumpy clouds are moving randomly in the gravitational field of the central SMBH, and are photoionized by the strong AGN emission. Estimates of the total mass of BLR clouds range from a few to a few thousand $M_\odot$, with densities from 10^9 to 10^{11} cm^{-3} (Baldwin et al. 2003). Even though the BLR is unresolved with current observational facilities, the size of the region can still be estimated from its variability, i.e. from reverberation mapping (see e.g. Botti et al. 2008), based on monitoring the variation of the strength of BLR emission lines as a function of corresponding changes in the photoionizing flux from the nucleus. Furthermore, recent studies have shown that the radius of BLR correlates with the L_λ(5100 Å) luminosity of AGN (Kaspi et al. 2005).

The Coronal Line Region (CLR), consisting of coronal emission lines from highly ionized species, is most likely located between the BLR and the NLR. This is supported by the fact that coronal lines are broader and blueshifted relative to narrow lines, and the suggestion that the clouds in CLR are outflowing material originating from the molecular torus (e.g. Rodriguez-Ardila 2002). However, it has also been proposed that CLR lines originate from the inner edge of the molecular torus (Pier & Voit 1995), although recent observations (Portilla et al. 2008) suggest that the CLR

emission region is spatially extended. The densities of the coronal clouds range from 10^2 from $10^{8.5}$ cm^{-3} (Ferguson et al. 1997). The CLR possibly contains several components (Murayama & Taniguchi 1998), such that the CLR clouds with the broadest emission lines are photoionized by nuclear UV radiation, whereas the more extended clouds with narrower emission lines are ionized by ambient shocks.

A molecular torus is the most important ingredient in the currently popular unification models, allowing an orientation-dependent effect by preventing an unobscured view to the central region. The torus is most likely composed of high density dust clouds in order to contribute enough extinction. It can not lie very close to the central engine, because otherwise its intense radiation field would dissociate the molecules and sublimate the dust. Most likely, the torus is assembled from dust clouds at high temperature (T ~ 1300 K) and the radius of its inner edge is ~1 pc (Krolik & Begelman 1988). The torus also gives rise to molecular line emission and near-infrared radiation (e.g. Pier & Krolik 1993). Although there is no direct observational evidence of the torus, e.g. the VLBI measurements of maser emission and interferometric mid-infrared observations of the of NGC 1068 (Greenhill et al. 1996, Jaffe et al. 2004) are consistent with a molecular torus at a radius of ~1 pc. The typical column density of the obscuring material in Seyfert galaxies is N(H) ~10^{24} cm^{-2} and a typical overall mass ~10^4 $M_\odot$ (Pier & Krolik 1992).

Unlike in the case of the BLR, the emission lines from the NLR are observable in both Type 1 and Type 2 AGN, with typical line widths of a few hundreds of kms^{-1}, indicating that the clouds are extended farther away from the nucleus and thus are less obscured than those in the BLR. The radius of the NLR is one magnitude larger than that of the BLR, ranging from ~10 to ~100 pc. The gas clouds in the NLR are usually photoionized by the nuclear source, but however, especially in Seyfert 2 galaxies and LINERs, they can also be ionized locally by hot OB stars. Electron temperatures of the NLR clouds are ~20000 K with densities in the range of $10^3 – 10^6$ cm^{-3}, but the NLR contains significantly more mass than the BLR, up to 10^9 $M_\odot$ in the most luminous quasars. The NLR extends in some AGN into an extended NLR (ENLR), reaching distances up to ~10 kpc from the center.

Finally, AGN are hosted in galaxies which span a continuum of morphologies from pure ellipticals to late-type spirals. The formation and co-evolution of the AGN and their host galaxies is currently a very active research field. AGN host galaxies are discussed in more detail in Chapter 4.

Fueling of the SMBH

The accretion mechanism powering the central engine in AGN requires a gas supply, without which the SMBH will remain dormant. Where does the infalling gas come from, and how does it end up in the vicinity of the SMBH? A longstanding controversy over the energy production by the accretion process has been the difficulty to find evidence for infalling gas flows because, most likely, the kinematics of the central regions of AGN is dominated by outflow motions (Crenshaw et al. 2003, Crenshaw & Kraemer 2007). However, recent observations of LINERs (e.g. Storchi-Bergmann et al.

2007) have indeed revealed the inward motion of gas toward the nuclear region.

The most crucial step in fueling the nucleus is for the accumulated gas to lose its angular momentum. There is no single mechanism that can accomplish that from kpc to sub-pc scales, but instead a variety of mechanisms must be invoked, such as gravitational torques, dynamical friction, hydrodynamical torques and viscous torques. The efficiency of a given mechanism depends on the distance from the nucleus, for instance gravitational torques provide the most efficient mechanism on scales from tens of kpc to a hundred pc.

Gravity torques induced by a large scale bar structure can generate a gas flow into the inner few hundred pc (Hernquist 1989, Mihos & Hernquist 1996), but can not drive gas closer than the Lindblad resonances where it will accumulate, often resulting in a star forming ring. It has been suggested that a nuclear (secondary) bar (or nuclear spirals) residing within the large scale (primary) bar could drive inwards of the Lindblad resonances (e.g. Shlosman et al. 1989, Maciejewski & Sparke 2000). Direct observational evidence of a nuclear bar driving gas into the inner region (< 100 pc radius) is seen e.g. in NGC 2782, containing a powerful circumnuclear starburst region (Jogee et al. 1999). Seyfert galaxies appear to have a slight excess of bars compared to inactive galaxies (e.g. Laine et al 2002). However, the role and importance of bars in the fuel transport is still controversial, as some studies do not show a correlation between AGN activity and the existence of bars (Mulchaey & Regan 1997).

In addition to non-axisymmetric gravitational fields, close interactions and minor mergers of galaxies (e.g. Tacconi et al. 1999, Cavaliere & Vittorini 2000, Scharwächter et al. 2004) may also provide a driving mechanism for inflowing gas. Indeed, numerical simulations have shown that gas flows induced by mergers are plausible to trigger AGN activity (e.g. Mihos & Hernquist 1996, Struck 1997). However, no correlation has been found between recent minor mergers and Seyfert-like activity (Corbin 2000). Nevertheless, interactions can not be ruled out as a cause for gas inflow, because there may be a long time delay between the triggering and the onset of the nuclear activity (e.g. Byrd & Valtonen 2001). This is supported by the lack of evidence for merger-related disturbed host galaxy morphology in AGN (e.g. Grogin et al. 2005, Gabor et al. 2009). However, shells and tidal tails have been observed in some early type AGN hosts (Bennert et al. 2008) indicating that they have undergone a relatively recent (a few hundred – Gyr) merging event.

The large and small scale environment of AGN can potentially shed light to the question of triggering the nuclear activity. For instance, the environments of Seyferts have been studied for a long time, but the results remain contradictory. Some studies have found evidence for an excess of companions in Seyferts compared to inactive spirals (e.g. Dahari et al. 1984, Rafanelli et al. 1995), while others have found no statistical difference (e.g. Laurikainen & Salo 1995, Schmitt 2001). Possible explanations for the discrepant results are biases in sample selection or a significant time delay before the onset of activity after the perturbation (Byrd & Valtonen 2001).

3.4 AGN classification

As was stated above, AGN are found to exist with many types of observed properties and in a wide variety of galaxies from late-type spirals to giant ellipticals. Therefore, to understand the formation and evolution of the AGN phenomenon, classification of the large number of different types of AGN is necessary. AGN can be classified in a variety of ways, e.g. based on the broadness of their optical emission lines, the brightness of their radio emission, or their variability properties. The main AGN classes that are discussed below are: LINERs, Seyfert galaxies, radio galaxies, quasars and blazars. Typical optical spectra of the different AGN classes are shown in Fig. 7.

Seyfert galaxies

Seyfert galaxies are low luminosity, radio-quiet objects which are typically hosted by a spiral galaxy. A few per cent of local spirals observed in the optical show the properties of Seyferts (e.g., Huchra & Burg 1992, Ho et al. 1997). Unlike their inactive counterparts, Seyfert galaxies show strong emission lines of high excitation in their nuclear spectra, and based on their appearance they are divided into Seyfert 1 and Seyfert 2 galaxies (Khachikian & Weedman 1974). Two types of emission lines can be observed: narrow and broad lines with velocities of a few hundred kms^{-1} and $10^3 – 10^4\,kms^{-1}$, respectively. The nominal velocity limit between narrow and broad lines is set at $1000\,kms^{-1}$. Forbidden emission lines, for instance [OIII] λ5007 Å, originating from low density gas (with electron density $\sim 10^3 – 10^6\,cm^{-3}$) are narrow in all Seyfert galaxies. On the other hand, permitted emission lines, such as Hα λ6563 Å, radiated from denser gas ($> 10^9\,cm^{-3}$), are either broad (in Seyfert 1 galaxies) or narrow (in Seyfert 2 galaxies). The different velocities indicate that the narrow and broad emission lines originate from different regions. The broad lines are emitted by gas clouds in the Broad Line Region (BLR) where the gas is photoionized by radiation from the accretion disc near the supermassive black hole, whereas the narrow lines originate further away from the center, in the Narrow Line Region (NLR) (see Section 3.3). The line widths are caused by Doppler broadening, as gas clouds move at high velocities around the nucleus. Based on whether the broad component can be seen in either or both of Hα and Hβ λ4861 Å, Seyfert 1s are further divided into three subcategories, namely Seyfert 1.5s (equally strong Hα and Hβ), 1.8s (Hα and weak Hβ) and 1.9s (only Hα) (Osterbrock 1981). Seyferts and their star forming activity have been recently widely studied especially in the infrared (e.g. Reunanen et al 2002, 2003).

LINERs

With increasingly accurate spectroscopic observations, a significant fraction of spiral galaxies (~30 %; Ho et al. 1997) show in their nuclei strong narrow and low ionization

emission lines (e.g. [OI] λ6300 Å, [SII] λ6731 Å) while high ionization lines (e.g. [OIII] λ5007 Å) are weak, leading to different emission line ratios than those found in both Seyferts and star forming galaxies (e.g. Veilleux & Osterbrock 1987). These galaxies are known as Low Ionization Nuclear Emission-line Regions (LINERs; nomenclature by Heckman 1980), and they are often considered to be low luminosity Seyfert galaxies. It is, however, possible that at least some LINERs are not AGN at all, but that their activity originates rather from a central star forming region. Thus, they may be transitional objects between high luminosity AGN, such as Seyferts, and lower activity galaxies. The emission line ratios of transition LINERs are between nuclear HII regions and pure LINERs (Ho et al. 1993). The majority of them show strong star formation (Cid Fernandez et al. 2004), which may also be the case in late-type pure LINERs (Alonso-Herrero et al. 2000). Note, however, that the definition of a LINER is rather arbitrary, and there is a continuous change in emission line properties from high luminosity Seyferts to low luminosity LINERs.

Radio galaxies

In the Papers below, the main focus will be on higher luminosity AGN, namely radio galaxies, BL Lac objects and quasars. Radio galaxies are typically giant (but otherwise normal) elliptical galaxies characterized by large extended (on a few hundred kpc – a few Mpc scales) radio emission lobes on opposite sides of the nucleus, originating from non-thermal synchrotron radiation. Based on their extended radio morphology (see Fig. 6), they are divided into two categories, FR-I and FR-II radio galaxies (Fanaroff & Riley 1974). FR-IIs have higher radio luminosity and are hosted by giant elliptical galaxies, whereas FR-Is have lower radio luminosity and are hosted by luminous cD galaxies (Owen & Laing 1989). At constant radio luminosity, FR-II host galaxies tend to be more luminous than FR-I host galaxies, although there is a large overlap (Ledlow & Owen 1996).

The radio emission in FR-II galaxies originates from an extended region farther away from the nucleus (edge-brightened), whereas in FR-I galaxies it comes from a region closer to the nucleus (edge-darkened). The lobes often have hot spots which are intensity peaks toward the outer edges of the lobes, where the jet hits the ambient medium and the kinetic energy of the jet is converted into random motion (Blandford & Rees 1974). The lobes of FR-II galaxies are often of very different brightness, or even one-sided. The nucleus is often connected to one or both radio lobes by a relativistic radio jet, transporting energy from the nucleus to the extended emission regions. In FR-I galaxies the jets are smooth, while in FR-II galaxies they have more knotty structure. Based on their optical emission line widths, radio galaxies are divided into broad (BLRG) and narrow line radio galaxies (NLRG), similarly to the case of radio-quiet Seyfert 1 and 2 galaxies.

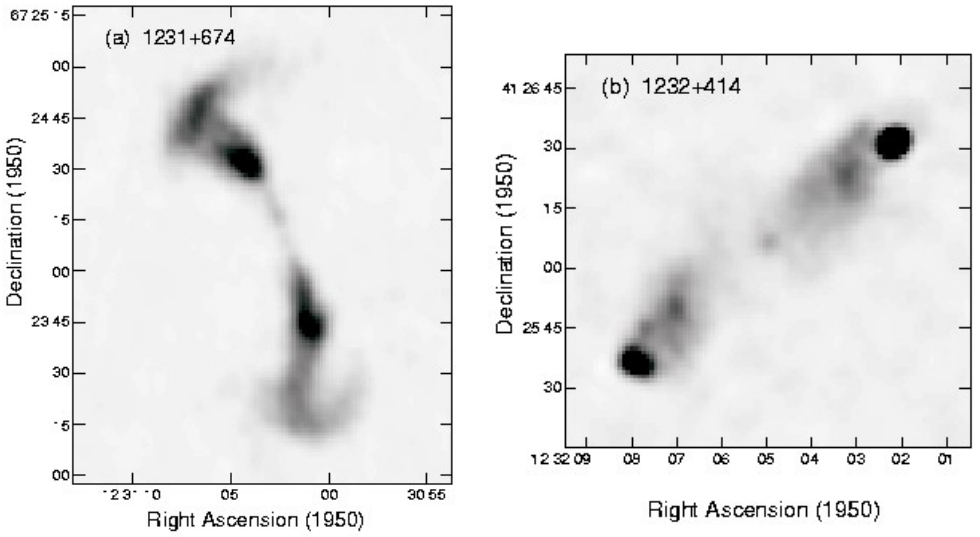

Figure 6: Radio images of two radio galaxies. a) FR-I radio galaxy 1231+674 with jets brighter close to the nucleus. b) FR-II radio galaxy 1232+414 with bright hot spots. (Courtesy of Frazer Owen and Mike Ledlow)

Quasars

Quasars (quasistellar radio sources) or QSOs (quasistellar objects) are the most luminous objects in the AGN zoo, showing both broad and narrow (Type 1) or only narrow (Type 2) emission lines in their optical spectra. High redshift Type 2 radio-quiet quasars, however, are difficult to identify. Because of their high obscuration, they have not been detected in UVX and emission line surveys, but their existence is necessary to explain the cosmic X-ray background (e.g. Gilli et al. 2007). They have indeed recently been found in increasing numbers, mostly through X-ray surveys (e.g., Beckmann et al. 2006, Sazonov et al. 2007), mid-infrared color surveys (e.g. Martinez-Sansigre et al. 2006, Polletta et al. 2008), and optical emission line surveys (Reyes et al. 2008), and currently more than 800 examples have been identified. Furthermore, Type 2 quasars might also be buried in a fraction of ultraluminous infrared galaxies (Franceschini et al. 2000).

The strong permitted broad emission lines (especially from hydrogen) indicate the presence of a similar BLR in quasars as in Seyfert galaxies. Indeed, based on the similarity of their observed spectra, quasars can be considered as high luminosity Seyfert galaxies with the dividing luminosity limit set at $M_V = -23.5$. However, it is only an arbitrary limit for classification purposes, without any astrophysical justification.

Although quasars were originally discovered based on their radio luminosity, only ~10 % of all quasars are radio-loud objects. The large majority of quasars are

radio-quiet, although not radio-silent, because there is a continuous distribution in their level of radio emission (Sanders et al. 1989). Radio-loud quasars are divided into the classes of lobe-dominated Steep Spectrum Radio Quasars (SSRQ) and core-dominated Flat Spectrum Radio Quasars (FSRQ), depending on the shape of their radio continuum. Similarly to FR-II radio galaxies, radio-loud quasars show often only one sided radio lobe and/or radio jet (Bridle et al. 1994).

Quasars have been found to exist over a wide redshift range, from nearby ($z < 0.1$) to high redshift objects (up to $z \sim 6.4$). The quasar population shows strong cosmological evolution, with the co-moving space density of quasars showing a broad peak at redshift $z \sim 2 - 2.5$ (Maloney & Petrosian 1999). This epoch is broadly coincident with that of the maximum in the cosmic star formation history (e.g. Madau et al. 1998, Franceschini et al. 1999, Shankar et al. 2009). However, even during this so called quasar epoch, they were hundreds of times less common than their inactive counterparts, and currently there is only ~1 quasar found for each 10^5 inactive galaxies.

BL Lac objects and OVV quasars (Blazars)

If the relativistic jet in a radio-loud quasar is oriented close to the line-of-sight of the observer, its luminosity will be Doppler-boosted by a very large factor (100 – 1000 times), and the non-thermal synchrotron emission from the jet will dominate over all other emission sources. Such quasars are called BL Lac objects, named after the first such object detected, BL Lac, in the constellation of Lacerta, that was previously thought to be a variable radio star (Oke & Gunn 1974). All AGN are variable at all wavelengths, but BL Lac objects are characterized by very highly variable emission on timescales as short as a day (and more commonly from days to to weeks), indicating that the prodigious energy comes from a very small, only light-day sized region. They also have high, variable polarization, smooth featureless optical spectrum with no or very weak emission lines (equivalent widths EW < 5 Å), and superluminal motion are observed in the radio wavelengths.

BL Lac objects are found either in radio (RBL) or X-ray (XBL) surveys. RBLs are typically more luminous and variable than XBLs (Jannuzi et al. 1994), and at first they were considered to belong to different classes of objects. However, later it was realized that the observed differences are due to their different synchrotron cut-off frequency, and RBLs and XBLs are now more commonly classified as low-frequency peaked (LBL) and high-frequency peaked (HBL) BL Lacs, respectively (Padovani & Giommi 1995). OVV (Optical Violently Variable) quasars are flat spectrum radio quasars which share many properties (such as variability) with BL Lac objects, but they additionally show broad emission lines in their spectrum. In fact, BL Lac objects and OVVs are commonly grouped together into a class of blazars.

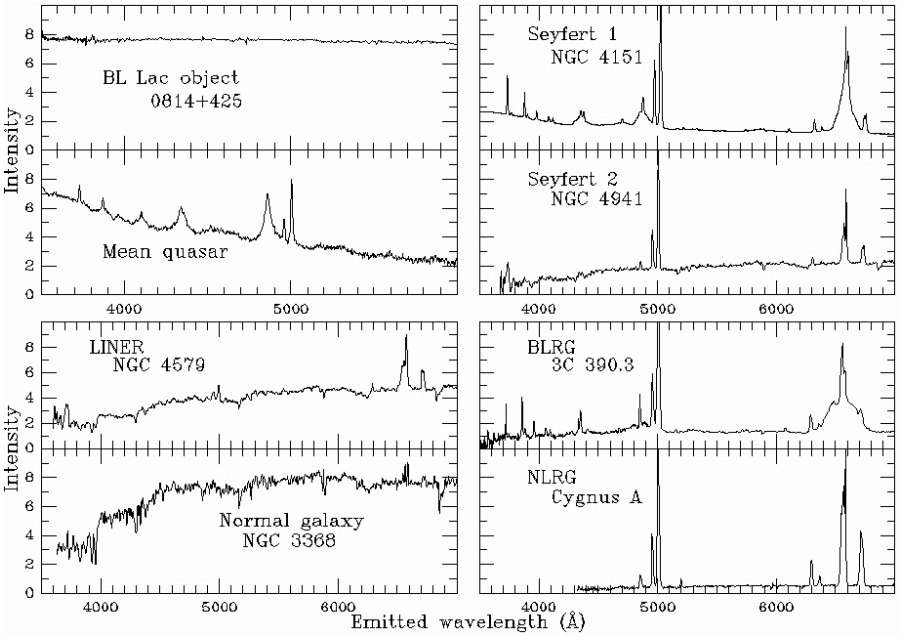

Figure 7: Typical optical spectra of different types of AGN and, for comparison, the spectrum of an inactive early-type galaxy (bottom left-hand corner). Note that the spectrum of the BL Lac object is nearly featureless. (Courtesy of Michael Richmond)

Summary

Even though the class of AGN contains many different kinds of objects with a wide range of observed properties (see Fig. 7), these objects need not be intrinsically different. Indeed, several types of unified models have been proposed, which seek to unify the observed properties mainly depending on their different orientation with respect to the observer. The unification of AGN is further discussed in Section 3.5.

3.5 Unified models

Even though there is a large number of observed AGN classes, it is possible and even likely that the appearance of a given type of AGN depends on our viewing angle. Therefore, unification is crucial to separate intrinsic properties of AGN from apparent, orientation-dependent ones, and thus to develop a deeper understanding of the underlying physics involved (e.g. Orr & Browne 1982, Urry & Padovani 1995).

As was mentioned above, Type 2 AGN have been classified as objects that show only narrow emission lines in their optical spectra. However, broad emission

lines have been observed in dozens of Seyfert 2 galaxies in polarized flux (e.g. Antonucci & Miller 1985, Miller et al. 1991, Tran et al. 1992, Moran et al. 2000, Gu & Huang 2002), showing that at least some Type 2 AGN also contain a BLR. Hot electrons below and above the plane of the molecular torus (shown as black dots in Figs. 5 and 8) scatter and polarize the broad lines and the nuclear emission into our line of sight. Note that scattered broad emission lines are not seen in every Seyfert 2 galaxy, suggesting that there are also intrinsic Seyfert 2s without a BLR (Osterbrock & Koski 1976, Tran 2001, 2003). However, broad emission lines have later been detected even in some of these cases in higher S/N polarized data or in infrared (e.g. Moran et al. 2001, Reunanen et al. 2003).

Although classification of AGN has traditionally been done based on optical spectroscopy, other wavelengths are also useful to probe the unification. For instance, in the infrared it is possible to study regions of galaxies affected by very high optical extinction ($A_V \sim 400$), although these still correspond to much smaller column densities than those found in the torus. Infrared spectroscopy has indeed revealed broad Brackett and Paschen lines in many Seyfert 2s (e.g. Lutz et al. 2002). Radio and hard X-ray observations are also useful because, similarly to infrared, they can penetrate through high column density material before being significantly absorbed. Seyfert 1s and 2s have similar radio luminosities (Rush et al. 1996) and the average extension of radio emission of Seyfert 2 galaxies is significantly higher than that of Seyfert 1's (Schmitt et al. 2001), consistent with predictions of the unified model. While the hard X-ray continuum in AGN arises from the accretion disc, soft X-rays are more easily absorbed by obscuring material and many Seyfert 2's show such prominent photoelectric cutoffs (e.g. Risaliti et al. 1999), confirming the existence of higher gas column densities in Seyfert 2 than in Seyfert 1s (Maiolino et al. 1998) in agreement with the unified model.

The above observations indicate that even though Type 1 and Type 2 AGN exhibit different properties, they might be physically similar objects. The unification models postulate that the appearance of an object depends crucially on whether the optically and geometrically thick molecular torus is seen face-on, allowing a direct unobscured view of the nuclear continuum and the BLR, or edge-on, with the view of the nucleus and the BLR obscured by the torus. For instance, Seyfert 1 galaxies are seen face-on, with broad emission lines, whereas in Seyfert 2 galaxies obscuration leads to the detection of only narrow emission lines.

In addition to the obscuring torus, another main determining parameter in standard unified models of radio-loud AGN is the orientation of the radio jet. If the object is viewed very closely along the jet, its radiation is dominated by synchrotron radiation from the jet, with nearly featureless spectrum, and it is classified as a BL Lac object. As the viewing angle increases, the appearance is that of a radio-loud quasar with one- or two-sided jet. When the viewing angle increases further, the extended radio emission lobes of radio galaxies are seen. Currently the most widely accepted unification of radio-loud AGN is based on the model of Urry & Padovani (1995), which unifies radio galaxies, radio-loud quasars and blazars. In this model, BL Lac objects are unified with FR-I radio galaxies, flat spectrum radio quasars with FR-II radio galaxies oriented at small jet angles (<15 deg) to our line of sight, while steep spectrum radio quasars are FR-II radio galaxies at larger jet angles (15 – 45 deg) (see

also Barthel 1989). The schematic view of this unification model is presented in Fig. 8.

If the unification is the correct model, unified objects should exhibit similar orientation-independent properties, such as extended radio emission (Urry & Padovani 1995, Willott et al. 2000), narrow line emission (Jackson & Browne 1990, Hes et al. 1993), isotropic infrared radiation from the torus (Heckman et al. 1994), host galaxies and luminosity functions (Urru & Padovani 1995), and large scale environments (e.g. Wurtz et al. 1997). Although the comparison is complicated by selection effects, the radio luminosities of FR-II galaxies and FSRQs and SSRQs are generally in agreement. The infrared radiation from the torus and the emission from the narrow line region radiate isotropically and thus, according to the unification model, they should be similar in radio galaxies and radio-loud quasars. However, infrared radiation seems to be stronger in quasars than in radio galaxies (Heckman et al. 1994). The [OII] line luminosities of quasars and radio galaxies appear to follow a similar distribution (Hes et al. 1993) but, however, the [OIII] emission line seems to be stronger in quasars (Jackson & Browne 1990). The luminosity functions of radio-loud quasars and radio galaxies appear to be in agreement, although their determination is made difficult due to several adjustable parameters, such as the source evolution.

Even though the unified model is capable of explaining most of the observed properties of AGN, it still has some persistent problems in addressing, e.g. the large scale environments, the sizes of the extended radio emission and the outflow velocities. FR-I radio galaxies are suggested to be the parent population of BL Lac objects but their environments appear to be different, such that FR-Is are located more frequently in clusters of galaxies than BL Lacs (Ledlow & Owen 1996, Wurtz et al. 1997). The Seyfert 1/Seyfert 2 ratio and the equivalent width of the CIV λ1549 Å emission line decrease with increasing luminosity, known as the Baldwin effect, contrary to the predictions of the unified model (Baldwin 1977, Kinney et al. 1990, Veilleux et al. 1999). These may be caused by luminosity-dependent opening angle of the torus (e.g. Elvis 2000). Perhaps the most obvious incompleteness of unification based on orientation concerns the radio-loud/radio-quiet quasar dichotomy. It is likely that the level of radio emission is a fundamental parameter related to the physics of AGN, and thus to explain the dichotomy, an additional parameter is unavoidable, such as black hole spin (Blandford 1990, Wilson & Colbert 1995), host galaxy morphology (Smith et al. 1986), or the nuclear feeding rate (Rees et al. 1982).

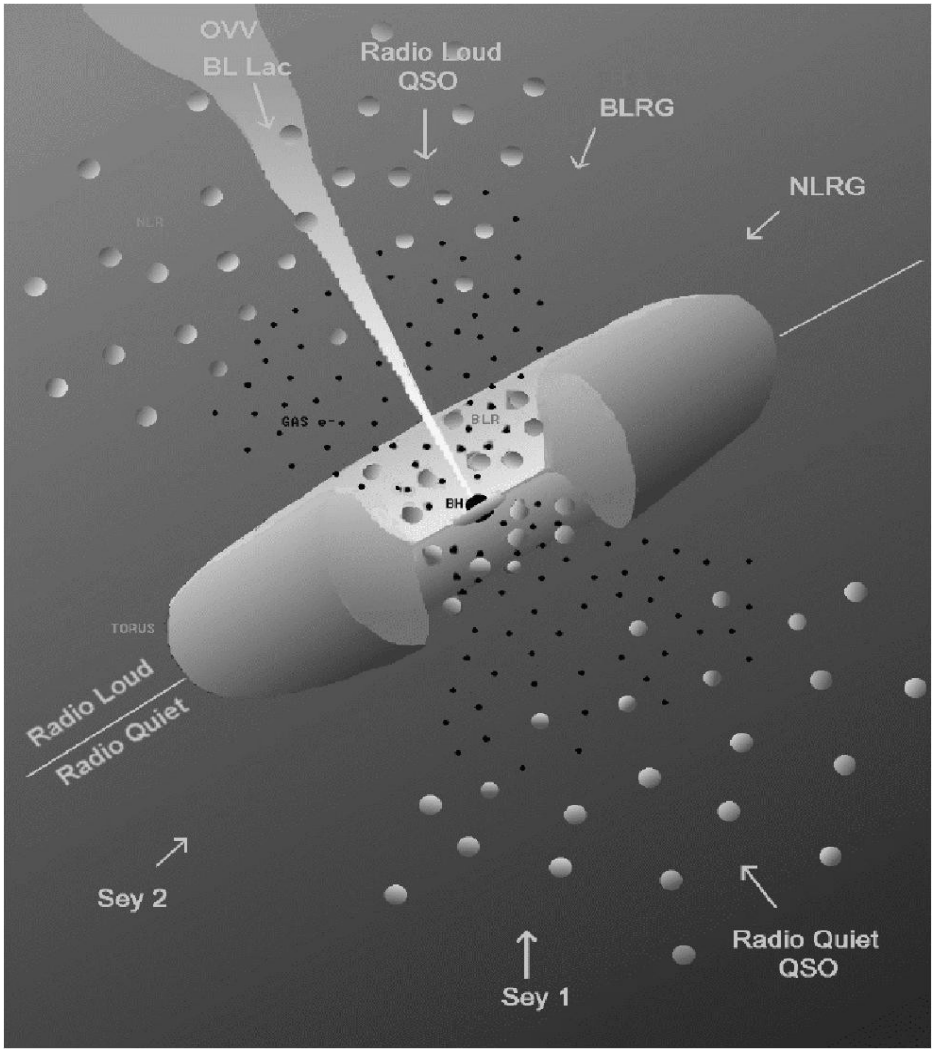

Figure 8: A schematic view of the unification model of AGN, showing the classification from different viewing angles. (Urry & Padovani 1995)

CHAPTER 4

The host galaxies of AGN

Does the nuclear activity depend on the properties of the underlying host galaxy, or vice versa? Is there a fundamental difference between the host galaxies of radio-loud and radio-quiet AGN? Although a certain answer to these questions eludes us, it has, however, recently become clear that the majority, if not all, nearby galaxies contain a SMBH in their center, indicating a co-evolution of the BH and the galaxy bulge. The investigation of AGN host galaxies is a crucial ingredient to understand the link between the evolution of galaxies and that of the nuclear activity. On the other hand, considering the unification of AGN, it is important to observe properties that are orientation independent, such as host galaxies. Unfortunately, especially going to higher redshift objects, it becomes a difficult task to extract and identify the underlying host galaxy under the bright central point source.

4.1 The extraction of AGN host galaxy

The image of an active galaxy is a superposition of two components, namely the (usually) luminous nuclear point source (AGN), and the (usually) faint underlying host galaxy. In quasars, for instance, radiation is dominated by the nuclear source, which makes it challenging to extract and study the faint host galaxies, especially in the case of high redshift objects. Since the AGN is always unresolved, it can be modeled by the point spread function (PSF). It represents the 2D surface brightness profile of a point source as a function of detector characteristics and atmospheric seeing conditions. The PSF varies with time and over the field of view of the detector, and can be estimated from foreground stars in the field.

Resolving the host galaxy is difficult for two reasons. First, at least for distant objects, the host has only small angular size (typically only slightly larger than the seeing disc) and, second, there is a strong cosmological surface brightness dimming of the host, scaling as $(1 + z)^{-4}$. The most reliable host galaxy detection is achieved from deep imaging with high S/N ratio and low nucleus-to-host luminosity contrast. Near-infrared observations are preferable over optical observations to achieve the latter requirement, because starlight from host galaxies peaks there, while AGN have there a local minimum in their SED, as shown in Fig. 9. Furthermore, as emphasized above, extinction is much reduced at near-infrared wavelengths.

The host galaxy extraction can be performed in either one or two dimensions. In the 1D extraction, preferable to use when dealing with low S/N images, an azimuthally averaged surface brightness profile over all radii is obtained. The advantage of this method is that it is simple and quite robust, but as a drawback, not all spatial information in the image is used.

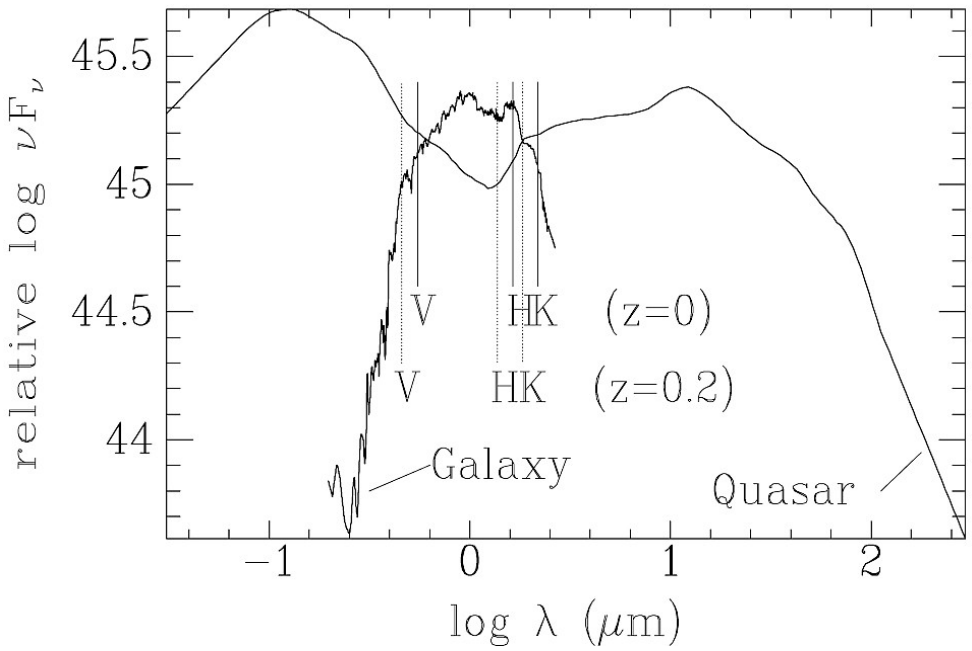

Figure 9: The optical V, and near-infrared H and K bands at redshifts z = 0, and z = 0.2, plotted over typical quasar and galaxy spectra. (McLeod & Rieke 1995)

To exploit all the spatial information, one needs to carry out full 2D analysis which employ simultaneous fitting of the nucleus and the host (e.g. McLure et al. 1999, Jahnke et al. 2004, Falomo et al. 2008). There are several 1D and 2D analysis algorithms employed in the literature (e.g. Peng et al. 2002, Kuhlbrodt et al. 2004). For the 2D analysis of radio-quiet quasars presented in this thesis (Paper II), the software package AIDA (Astronomical Image and Decomposition and Analysis: Uslenghi & Falomo 2007) was used, designed for 2D quasar host galaxy fitting.

For both 1D and 2D extraction procedures, the most critical task is the generation of a reliable PSF model. It is constructed from an average of both faint unsaturated star(s), to model the bright central part of the PSF, and bright saturated star(s), to represent the faint PSF wings. The accurate modeling of the wings is essential, because most of the signal from the host galaxy will be detected against this region of the PSF profile. The field stars used for the PSF generation are selected based on their FWHM, sharpness and roundness. If several stars are used in the modeling, distributed over the field, it also has to be confirmed that the resulting model is stable, with no significant variations between the profiles of individual stars.

The surface brightness of galaxies can be modeled by Sersic $r^{1/n}$ model (Sersic 1968) given as

$$I(r) = I_e exp\left\{-b\left[\left(\frac{r}{r_e}\right)^{1/n} - 1\right]\right\}$$

where I is the surface brightness of a galaxy, r_e is the scale length, i.e. the radius which encloses half of the total luminosity of the galaxy, and I_e is the surface brightness at the scale length radius. The parameter n gives the surface brightness distribution, varying from $n = 1$ to $n = 10$, and the parameter b is a function of n. There are two important special cases derived from the generic Sersic model that are widely used to model host galaxies, namely a de Vaucouleurs $r^{1/4}$ law (de Vaucouleurs 1948), and an exponential law (Freeman 1970) given as

$$I(r) = I_e exp\left\{-7.67\left[\left(\frac{r}{r_e}\right)^{1/4} - 1\right]\right\}$$

$$I(r) = I_d exp\left(-\frac{r}{r_d}\right)$$

In the latter equation, the r_d is defined by an equation $r_{1/2} = 1.68 r_d$. The de Vaucouleurs law is adequate for modeling of elliptical galaxies and bulges of spiral galaxies, whereas the exponential law is used for spiral galaxies.

Inactive early-type galaxies and bulges of spiral galaxies follow a tight relation between their scale length r_e, stellar velocity dispersion σ, and surface brightness μ, which is known as the 3D Fundamental Plane of elliptical galaxies (Dressler et al. 1987, Djorgovski & Davis 1987). It is related to a morphological and dynamical structure of galaxies. Considering only the surface brightness and the scale length, the projection is known as the Kormendy relation (Kormendy 1977, Kormendy & Djorgovski 1989), and it is well established for nearby cluster galaxies (e.g. Jörgensen et al. 1996).

The surface brightness models can also be applied to characterize the host galaxies of AGN. Although host galaxies span a continuum of morphologies, they are usually designated as spirals or ellipticals because the quality of data is not sufficient to determine the morphology at a greater level of accuracy. For the characterization of the AGN host galaxy, first the image of the AGN is fitted with the PSF model only, to indicate any deviations from a point source. If the observed profile deviates significantly from the PSF model, the source is evaluated as resolved and it is then simultaneously fitted with a scaled PSF (to model the nuclear component) and a scaled surface brightness model for the host galaxy, using either a de Vaucouleurs ($r^{1/4}$) bulge model or an exponential disc model. The fitting is performed by using an iterative least-squares fitting, minimizing its χ^2-value, and main parameters of the host galaxy, e.g. luminosity, central surface brightness and scale length, are derived from the fitting.

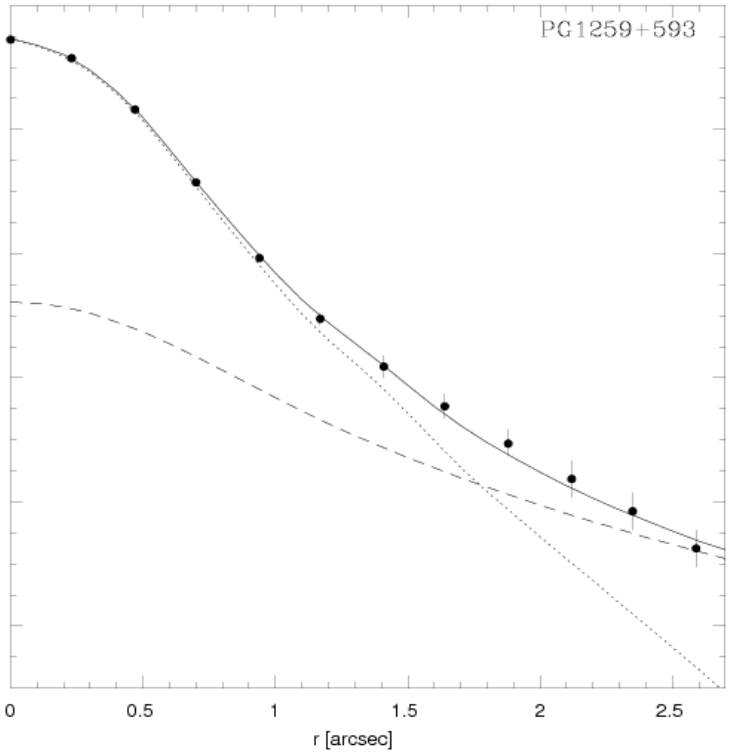

Figure 10: The azimuthally averaged radial surface brightness profile of the quasar PG 1259+593 (solid points with error bars) overlaid with the PSF model (dotted line), an $r^{1/4}$ de Vaucouleurs model for the host galaxy (long-dashed line), and the best-fit PSF+host galaxy model profile (solid line).

However, while integrated properties, such as the host galaxy luminosity, are relatively accurately determined, the scale length and the central surface brightness are often poorly constrained due to a degeneracy between the two parameters. As an example of the procedure, the 1D radial surface brightness profile of the resolved quasar PG 1259+593, overlaid with the PSF and de Vaucouleurs surface brightness models, is presented in Fig. 10.

4.2 Low redshift AGN host galaxies

A fundamental issue in the study of AGN and their host galaxies is to investigate the possible connection between the properties of the host galaxies and the nuclear activity. The most obvious question is how, if at all, the properties of AGN depend on the host galaxy morphology or vice versa. Moreover, because the central engine is very energetic, as manifested e.g. by the presence of outflowing jets in radio-loud AGN, one might assume that the AGN may induce disturbed morphology within the host galaxy. Unfortunately, our theoretical understanding of the evolution of galaxies is still limited, and hence arguments have to be based on empirical relations between the properties of AGN (e.g. radio emission, variability) and the host galaxies (e.g. luminosity, morphology, velocity dispersion).

Morphology and luminosity of hosts

Most of the work on AGN host galaxies has focused on determining their luminosities and morphologies. The first host galaxies of quasars were resolved already by Kristian (1973), but the next major step forward in the field had to wait until the late 1970's when the extended nebulosities around quasars were spectroscopically confirmed to be of stellar origin (Green et al. 1978, Boroson et al. 1982). Ever since, imaging and spectroscopic observations of low redshift host galaxies have been widely carried out, first mainly with optical CCD detectors, but nowadays increasingly in the near-infrared, thanks to the significant improvements in high sensitivity infrared detectors (e.g. McLeod & Rieke 1994a,b, Bahcall et al. 1997, Falomo & Kotilainen 1999, McLure et al. 1999, Hamilton et al. 2002, Dunlop et al. 2003, Pagani et al. 2003, Kotilainen & Falomo 2004, Floyd et al. 2004, Raimann et al. 2005).

Radio-loud AGN are relatively rare (~10% of all AGN) compared with their radio-quiet counterparts. However, radio emission itself is a fundamental physical parameter of AGN, and consequently it is important to determine whether there is any correlation between radio loudness and the host galaxy morphology. This issue was first studied by Adams (1977) who found that radio-loud AGN (e.g. radio galaxies) occur most frequently in elliptical galaxies, whereas radio-quiet AGN (e.g. Seyferts) are mostly found in spiral galaxies (see also e.g. Ho et al. 1997). It is evident, however, that these early host galaxy studies had biased sample selection. Based on a radio-selected, unbiased sample, more recently, Martel et al. (1998) showed that a large majority (~80 %) of nearby 3C radio-loud AGN reside in elliptical galaxies. This is in stark contrast with the fact the majority of all galaxies are spirals, and clearly indicates a link between the formation of bulges and the nuclear radio emission.

Recent imaging studies have established that practically all luminous low redshift ($z < 0.5$) AGN, *independent of their radio loudness*, are hosted by luminous and massive elliptical galaxies (consistent with a de Vaucouleurs $r^{1/4}$ surface brightness law), whereas low luminosity radio-quiet AGN can also be found in early-type spiral galaxies, following an exponential disc law (Hamilton et al. 2002, Dunlop et al. 2003,

Pagani et al. 2003). For instance, the absolute *R*-band magnitude of radio-loud AGN hosts falls typically between M_R^* and M_R^*–2, where $M_R^* \sim -21.2$ (Gardner et al. 1997, Nakamura et al. 2003) is the characteristic luminosity of the Schecter luminosity function. The hosts of radio-quiet quasars appear to be less luminous than those of radio-loud quasars, with ~0.5 mag difference reported in the literature (e.g. Kirhakos et al. 1999, Hamilton et al. 2002, Dunlop et al. 2003).

On average, the host galaxies are large, with typical scale length of $r_e = 5 - 15$ kpc (e.g. McLure et al. 1999, Dunlop et al. 2003), much larger than that of inactive ellipticals, where ~3 kpc marks the boundary between normal and giant ellipticals (Capaccioli et al. 1992). Furthermore, low redshift quasar hosts are consistent with the Kormendy relation between scale length and surface brightness of inactive elliptical galaxies (e.g. McLure & Dunlop 2002, Kotilainen & Falomo 2004). This indicates that the dynamical structure of AGN hosts is similar to their inactive counterparts, thus suggesting that the AGN has an insignificant influence to the global structure of the underlying galaxy.

Although quasars are rare in the local Universe, recent observations (e.g. Ferrarese 2006 and references therein) have confirmed the existence of a (dormant) SMBH in the center of the large majority (if not all) of low redshift inactive elliptical galaxies. There is a relatively tight linear correlation between the black hole mass, and the luminosity and the stellar velocity dispersion of the galaxy bulge (e.g., Kormendy & Richstone 1995, Ferrarese & Merritt 2000, McLure & Dunlop 2002, Häring & Rix 2004, Ferrarese 2006). This relation indicates that the formation and evolution of the bulge and the SMBH are closely linked. The same relation has been found to hold also for AGN (e.g. Laor 1998, McLure & Dunlop 2002, Wandel 2002). In fact, the most powerful AGN are found exclusively in the most luminous (massive) galaxies (Falomo et al. 2003, Kauffmann et al. 2003), suggesting that every massive galaxy may undergo one or several transient active phases in its evolutionary history, with power that depends both on the mass of the SMBH (and therefore, on the mass of the galaxy) and the amount of gaseous material for fueling.

As was stated in the previous chapter, radio emission is a fundamental physical feature of AGN independent on the viewing angle. There is increasing evidence that radio-loud AGN contain systematically more massive BHs than their radio-quiet counterparts (e.g. Laor 2000, McLure & Dunlop 2001b, Dunlop et al. 2003, McLure & Jarvis 2004, Metcalf & Magliocchetti 2006). Indeed, it has been postulated (Laor 2000) that radio emission could also depend on the mass of the central SMBH, with a threshold level of black hole mass for the onset of powerful radio source, and a smaller threshold mass for sustaining a radio-quiet AGN. These mass thresholds then translate into bulge luminosities that are ~0.7 mag brighter for radio-loud quasars, in agreement with imaging results (see references above). The scarcity of massive galaxies in the elliptical galaxy luminosity function then leads naturally to the observed factor of ten difference in the number density of radio-loud and radio-quiet quasars (Dunlop et al. 2003). However, it has to be kept in mind that there is a large overlap in the distributions of radio-loud and radio-quiet AGN, e.g. in their accretion rate and host galaxy morphology, and that the measurements of black hole masses may suffer from selection effects (e.g. Ho 2002). Therefore, BH mass alone is insufficient to explain the

radio-loud/quiet dichotomy, but one or more additional physical parameter(s), such as the spin of BH or evolutionary effects, are necessary (McLure & Jarvis 2004).

The colors and spectroscopy of host galaxies

While single filter observations are able to derive the host galaxy morphology and luminosity, they do not tell anything about their SED. The large majority of host galaxy imaging studies have been traditionally carried out in only in one wavelength, typically in the optical *R*-band, while only recently studies have been made in multiple filters, addressing the colors of the host galaxies (Dunlop et al 2003, Jahnke et al. 2003, 2004, Kotilainen & Falomo 2004). Stars of different age and metallicity dominate the stellar populations at different wavelengths, and thus to trace the contribution from various stellar populations to the observed SED of the hosts, it is crucial to obtain multicolor imaging both in the optical and near-infrared. While imaging cannot compete with spectroscopy in terms of spectral resolution, its advantage is its robustness, being less affected by nuclear contamination to the host galaxy flux than especially low spatial resolution spectroscopy.

Although Dunlop et al. (2003) found quasar $R - K$ host colors to be similar to those of massive ellipticals, there is nowadays increasing evidence that AGN hosts appear to be bluer with a wider dispersion than inactive early- and late-type galaxies (Schade et al. 2000, Jahnke et al. 2004, Kotilainen & Falomo 2004, Sanchez et al. 2004), and furthermore they do not follow the color-magnitude relation of inactive ellipticals (Peletier et al. 1990). For example, Fig. 11 shows the $R - H$ colors of AGN hosts as a function of their *H*-band absolute magnitude, compared with the color-magnitude relation of inactive early-type galaxies. The blue colors most likely indicate that the host galaxies have undergone a relatively recent star formation episode, while the wide color dispersion suggests large object-to-object variations in time since the latest star formation episode. Recent spectroscopic observations support this multicolor view, that a significant fraction of AGN hosts contain two stellar population components, namely the old stellar component that dominates the integrated luminosity, and an additional intermediate age (~2 Gyr) stellar component (Raimann et al. 2005).

Especially for tracing the young stellar population, optical spectroscopy in the blue domain is useful, whereas near-infrared spectroscopy, containing many diagnostic stellar spectral absorption features (see Section 2.6), is advantageous for tracing RGB (Red Giant Branch) stars that dominate the luminosity at 2 μm. Unfortunately, currently there are no self-consistent near-infrared synthetic spectral models for interpretation of the near-infrared absorption features, but instead one has to rely on the comparison of observed spectra with stellar atlases (e.g. Wallace & Hinkle 1996).

Spectroscopy of host galaxies is much more difficult than photometry, because one has to place the slit optimally in an off-nuclear position where there is enough flux from the host galaxy to perform stellar population analysis, and which is at the same time not overwhelmingly contaminated by the bright nuclear emission. The pioneering spectroscopy of quasar hosts was carried out by Boroson et al. (1985), while more

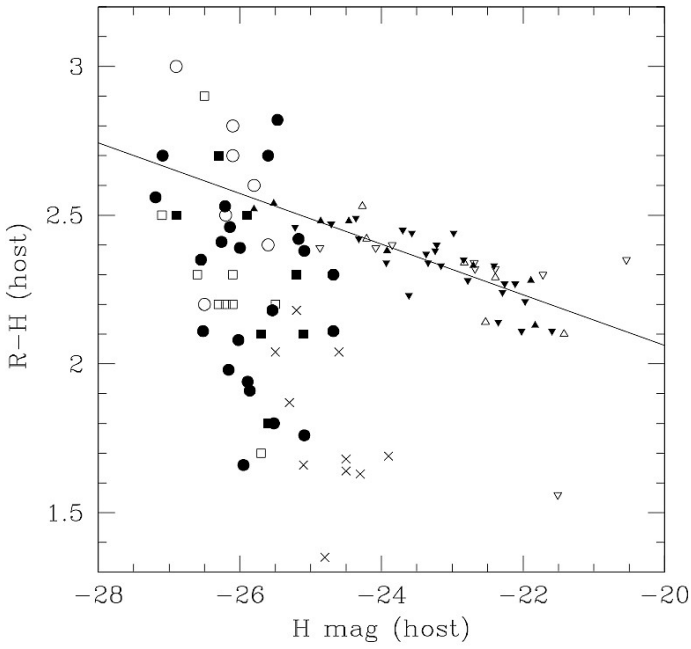

Figure 11: The R–H vs. M_H color-magnitude relation of AGN host galaxies. Filled and open circles and squares represent BL Lac host galaxies, crosses represent quasar hosts (Jahnke et al. 2004), filled, open and inverted triangles represent early-type galaxies from Virgo and Coma clusters (Bower et al. 1992a,b). The solid line is the best-fit regression of early-type galaxies. (Adapted from Kotilainen & Falomo 2004)

recent work in the field includes Hughes et al. (2000), Nolan et al. (2001), Jahnke (2002), Raimann et al. (2005), and Letawe et al. (2007). Hughes et al. (2000) and Nolan et al. (2001) found evidence from off-nuclear spectroscopy that quasar hosts were dominated by old stellar populations. On the other hand, Jahnke (2002) modeled on-nuclear spectra simultaneously into nuclear and host galaxy spectra, using information of the PSF shape and host galaxy parameters, and found predominantly young host galaxy ages. Together with results from broad-band colors (e.g. Kotilainen & Falomo 2004, Jahnke et al. 2004), this disagreement suggests the existence of two populations of quasar host galaxies, one blue and gas-rich, the other red and gas-poor.

Large scale environment and triggering

Another orientation-independent property of AGN, in addition to their radio emission, is their large scale environment. In general, galaxies reside in a large range of environments, from isolated galaxies via poorly clustered groups to large dense

clusters. The majority of luminous elliptical galaxies are found within clusters, while spirals are typically found in the outskirts of clusters (Dressler 1980, Balogh et al. 1998). It has been suggested that the radio loudness of AGN is a function of their environments (e.g. Yee & Green 1984, Ellingson et al. 1991). However, the role of the large scale environment to the evolution of AGN is still controversial, and it appears that it plays only a minor role in determining the radio luminosity. In fact, AGN seem to prefer poor groups of galaxies rather than the centers of high density clusters (Best 2004, Söchting et al. 2004), and no significant differences have been found between the environments of radio-loud and radio-quiet AGN (Wold et al. 2001, McLure & Dunlop 2001a).

The most likely triggering mechanism for the nuclear activity is either a major or minor merger of or milder interaction between gas-rich galaxies that drives gas into the central region where it can feed the SMBH. While interaction is expected to induce disturbed morphology within the galaxies, such as tidal tails, asymmetries and extended emission, the majority of AGN hosts appear to be ellipticals with smooth morphology (e.g. Jahnke et al. 2004, Villforth et al. 2008) indicating a significant time delay (several 100 Myr) between the merging event and the onset of the nuclear activity. On the other hand, there is some evidence for starbursts induced by tidal interactions (Canalizo & Stockton 2001) indicating a link between circumnuclear star formation and nuclear activity. Furthermore, Bennert et al. (2008) have found shells and tidal tails in some early type AGN host galaxies.

4.3 High redshift AGN hosts and their evolution

The evolution of galaxies can be probed by spanning their observations up to redshifts that cover the major part of the history of the Universe. Currently, the most distant galaxy has a redshift of $z = 6.96$ (Iye et al. 2006) corresponding to an age of the Universe of only ~0.8 Gyr. Note that the most distant quasar known is at very similar redshift, $z = 6.427$ (Willott et al. 2007). By observing galaxies within a large redshift range, it is possible to follow the evolution of galaxies e.g. in their luminosity, morphology, size, and activity level, giving a valuable insight also to the origin of the AGN phenomenon.

The morphology of high redshift AGN hosts

At high redshifts, resolving the host galaxy beneath the bright nuclear source is even more challenging than at low redshifts, due to the strong cosmological surface brightness dimming of the host in contrast to the nucleus, and requires very deep observations at very high spatial resolution. Thanks to recent improvements in telescope and detector technology, such as the large collecting area provided by the 10 meter class telescopes equipped with adaptive optics, have made it possible to extend the host galaxy observations up to considerably high redshifts.

The first high redshift AGN host galaxy studies were performed in the optical (e.g. Romanishin & Hintzen 1989, Hutchings et al. 1989), but currently, the emphasis is in the near-infrared, corresponding to rest-frame optical wavelengths (Falomo et al., 2004, 2005, 2008, Ridgway et al. 2001, Kotilainen et al. 1998a,b, 2006, 2007, Kotilainen & Falomo 2000, Kukula et al. 2001, Kuhlbrodt et al. 2005, Peng et al. 2006, Villforth et al. 2008, Schramm et al. 2008).

From the quoted studies, it has become clear that the host galaxies of both radio-loud and radio-quiet quasars at high redshift, similarly to their lower redshift counterparts, are luminous, large and massive galaxies, usually well consistent with a de Vaucouleurs luminosity profile. Furthermore, they are consistent with the Kormendy relation of ellipticals indicating that their structure is similar to the low redshift hosts. However, accurate determination of the morphology of the hosts is extremely difficult, because elliptical and disc profiles show largest difference at small radii and in the tail of the wings, that require very high quality data at high redshift to uncover.

The evolution of radio-loud and radio-quiet AGN hosts

The modern theory for galaxy formation is based on the widely accepted ΛCDM (Cold Dark Matter) model where CDM halos provided initial seeds for the structure formation. According to this model, gas falls into the dark matter halos, forming dense molecular clouds and finally stars. This model is considered as a hierarchical model (e.g. Kauffmann & Charlot 1998, Kauffmann & Hähnelt 2000, Di Matteo 2004), in which the smallest structures were formed first, and SMBHs in the centers of galaxies grew up due to major mergers. It provides a natural link between the mass growth of the SMBH in the galactic nucleus and the nuclear activity. It also indicates a strong decrease in the number density of bright AGN from $z = 2$ to present epoch due to the decrease of gas supply and the merger rate and, in addition, increase in the time scale of gas accretion. This is consistent with the observed strong peak in the density of AGN at redshifts $2 < z < 3$ (e.g. Dunlop & Peacock 1990, Boyle 2001, Nandra et al. 2005). Furthermore, according to the hierarchical model, the luminosity of galaxies increases towards lower redshifts due to merging.

The star forming history as a function of redshift modeled by hydrodynamic N-body simulations (Springel & Hernquist 2003) is presented in the left-hand panel of Fig. 12. The precise epoch of the peak in the star formation rate depends on the exact parameters of the model (e.g., Somerville et al. 2001, Nagamine et al. 2001, Ascasibar et al. 2002), but it occurs at the redshift range $3 < z < 6$. The increase of the star formation rate profile at very high redshifts is due to structural growth in the dark matter halos, whereas the decrease at low redshifts is caused by the decreasing density of cold gas.

This star formation model implies that half of the stars have formed before redshift $z \sim 2$ corresponding to an age of the Universe of only a few Gyr, while recent star formation is suppressed such that only ~25% of stars have formed at redshifts $z < 1$. The right-hand panel of Fig. 12 presents the mean and the median ages of stars compared with the age of the Universe. The mean age of stars increases very rapidly as

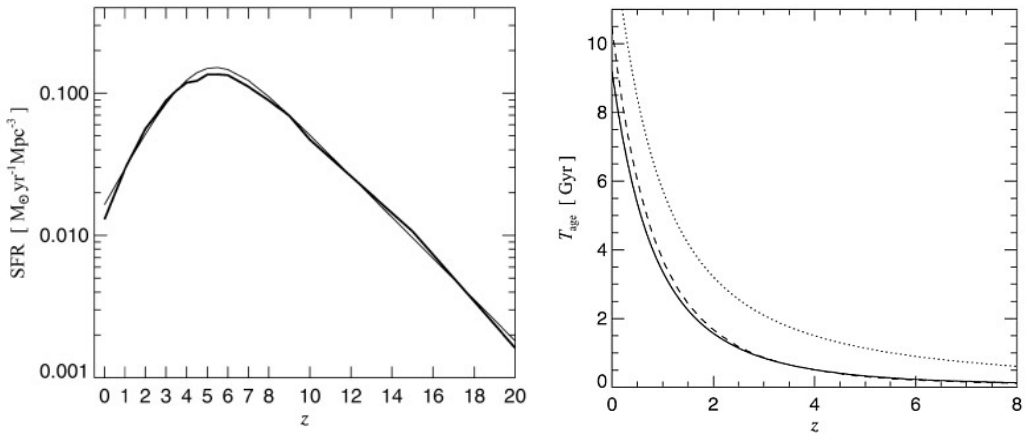

Figure 12: Left panel: Theoretical star formation rate density (thick line) derived by N-body simulation compared with analytical model (thin line). Right panel: Mean (solid) and median (dashed) ages of star shown together with age of the Universe (dotted) (Springel & Hernquist 2003).

the star formation rate decreases, and at the present epoch an old stellar population should have a mean age of ~9 Gyr. This scheme is, however, complicated by feedback from supernovae and AGN, which enriches the gas with heavier metals, and may even produce strong winds to sweep up the gas beyond the potential well of the nucleus. The original hierarchical model has difficulties to interpret the observed evolution of galaxies, and thus several modified models have been presented which include AGN feedback (Granato et al. 2004, De Lucia et al. 2006, Bower et al. 2006).

Currently, observations of AGN hosts have been carried out over a wide redshift range, from the present epoch up to $z \sim 3$ and even beyond. As was stated above, the co-moving space density of AGN peaks at $z \sim 2 – 3$, which agrees well with the star formation history in the Universe (e.g. Franceschini et al. 1999, Yu & Tremaine 2002, Marconi et al. 2004), suggesting a strong link between the formation of luminous galaxies and AGN activity. Therefore, host galaxy observations at redshifts near and beyond the AGN peak are crucial (Falomo et al. 2008).

The evolution of the host galaxies of both radio-loud and radio-quiet quasars at redshifts $0 < z < 3$ has been studied by Falomo et al. (2008) and their results are shown in Fig. 13. The hosts of radio-loud AGN are ~1.5 mag more luminous at $z \sim 3$ than the hosts at the present epoch. On average, their absolute magnitudes are in agreement with those of M_R^*–2 inactive galaxies undergoing simple passive evolution of massive spheroids. The evolution of the radio-loud AGN hosts over a wide redshift range follows a very similar trend to that of radio galaxies (Willott et al. 2003) suggesting they have a shared origin. Numerous imaging studies have shown that radio-loud and radio-quiet AGN hosts have similar morphology (e.g. Bahcall et al 1997, Dunlop et al

2003, Pagani et al. 2003, Kotilainen et al. 2007), and thus it is interesting to compare their evolution. Because of the correlation between the masses of the bulges and the SMBHs, such a comparison may give insight to the fundamental cause for their different radio emission properties. This comparison, presented in Fig. 13, has recently been performed by Falomo et al. (2008), and Kotilainen et al. (2009). Low redshift radio-quiet AGN hosts are ~1 mag fainter than those at redshift $z \sim 2$. The evolution of the radio-quiet AGN hosts appears similar to that of radio-loud AGN hosts, but the host galaxies of radio-quiet AGN appear to be systematically ~0.5 mag fainter than their radio-loud counterparts over the whole redshift range $0 < z < 3$, and are consistent with the luminosity of inactive elliptical galaxies at redshifts $z \sim 1.4$ and $z \sim 1.8$ (Longhetti et al. 2007, Daddi et al. 2005).

The evolution of both radio-loud and radio-quiet AGN hosts is in agreement with passive evolution of massive early-type galaxies, suggesting that their stellar population was formed at high redshift ($z > 3$) and evolved passively ever since. This scenario of old dominant stellar population is supported by spectroscopy of low redshift AGN (Nolan et al. 2001). However, it is inconsistent with the hierarchical model which predicts an increase of luminosity towards lower redshift due to merging events, while the current observations suggest that the hosts have experienced their last major merger at very high redshifts and are already fully assembled beyond the peak of the AGN activity (Kotilainen et al. 2009). Merging events at lower redshifts have insignificant contribution to the host luminosity.

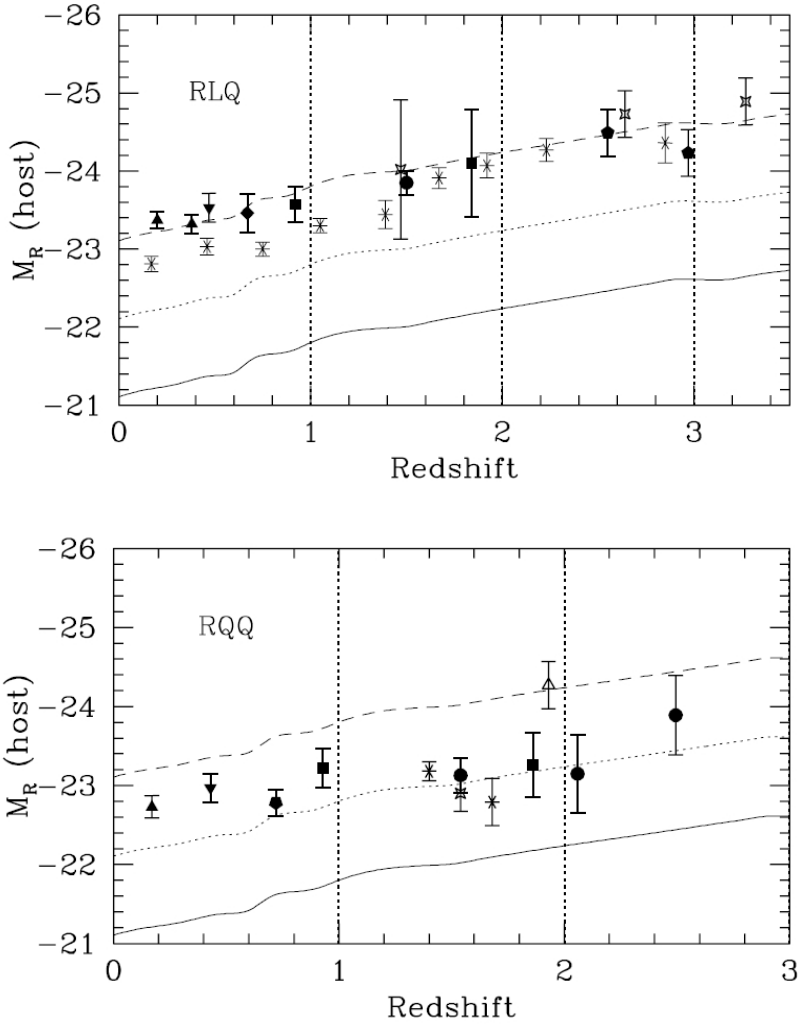

Figure 13: The luminosity evolution of the host galaxies of radio-loud (upper panel) and radio-quiet (lower panel) quasars, compared with passive evolution of massive M, M*–1, and M*–2 inactive ellipticals (solid, dotted and long dashed lines; Bressan et al. 1998). Upper panel: radio galaxies are shown as asterisks. Lower panel: Massive inactive early-type galaxies at z = 1.4 and z = 1.8 are shown as crosses. For the symbols of the various quasar samples, see Falomo et al. (2008). Symbols have been plotted at the average redshift of the sample. (Adapted from Falomo et al. 2008).*

CHAPTER 5

Future work

Recent imaging observations have shown that a significant fraction of AGN host galaxies are bluer than their inactive counterparts and, in addition, clearly do not obey the color-magnitude relation of ellipticals (e.g., Govoni et al. 2000, Kotilainen & Falomo 2004; Paper III). The blue host galaxy colors suggest that AGN hosts have experienced a relatively recent star formation episode, resulting in a young/intermediate age stellar population. In order to have a closer insight into their star formation history, spectroscopic observations are needed (c.f. Paper IV). To accomplish this goal, my next project is to characterize the stellar content and star formation history of the BL Lac host galaxies and, together with stellar population synthesis models, to estimate the ages of the stellar populations. These results will be used to assess whether the AGN hosts have experienced a relatively recent star formation episode, and whether the observed blue colors of the AGN hosts indeed are due to a young/intermediate age stellar population. This has important implications for understanding the connection between the star formation and the nuclear activity.

In fact, a pilot study of the BL Lac object PKS 2005-489 has shown the capability of such spectroscopic observations (Bressan et al. 2006). High signal-to-noise ($S/N \sim 300$) optical long slit spectra were obtained with the ESO VLT/FORS1 instrument, revealing an extended star forming region surrounding the nucleus. However, a larger sample is needed to reach any statistical conclusions. Towards this goal, our group has been granted observing time with the ESO VLT/FORS2 instrument to obtain optical (3300 – 8450 Å) spectra, covering wavelengths from the Balmer discontinuity up to the Hα emission region for five low redshift ($z < 0.1$) BL Lac host galaxies. Furthermore, we have recently been granted observing time for additional six BL Lac objects at the Palomar Observatory 5m Hale telescope and the DBSP spectrograph, to complete the sample.

The observed correlation between the mass of the central black hole, and the luminosity and stellar velocity dispersion of the host galaxy bulge (e.g., Ferrarese & Merritt 2000, McLure & Dunlop 2002, Häring & Rix 2004) suggests that the formation and evolution of galaxies and supermassive black holes are closely linked. A recent study of low redshift ($z < 0.6$) quasars (Labita et al. 2006) found that active galaxies obey a similar $L_{\rm bulge}$ - $M_{\rm BH}$ relation as inactive galaxies. However, this relation has only been studied for low redshift quasars, whereas the evolution of the relation over cosmic time is still largely uncertain. Actually, such a study has so far only been attempted by Peng et al. (2006) for a small sample of high redshift gravitationally lensed quasars. They found that the ratio between the masses of the black hole and the bulge significantly increases with redshift. It is essential to expand the study of the relation to higher redshifts and to larger samples. To this end, our group has projects underway to study the evolution of the relation in the redshift range $1 < z < 2.5$ (Decarli et al., in

prep.) and, in addition, to enlarge the amount of studied low redshift quasars to improve the statistics over the results of Labita et al. (2006). M_{BH} can be dynamically measured only for a limited number of nearby luminous galaxies, where the sphere of influence of the BH can be resolved. Fortunately, M_{BH} of even distant active galaxies can be estimated from the virial theorem using the equation: $M_{BH} = v^2_{BLR} R_{BLR} G^{-1}$, where v_{BLR} and R_{BLR} are the velocity and the radius of the BLR, respectively (Wandel et al. 1999, Vestergaard 2002). The velocity can be derived from the FWHM of the broad emission lines, assuming a specific geometry for the BLR, $v_{BLR} = f$ x FWHM where f is a geometrical factor. As was stated above, for nearby galaxies R_{BLR} can be estimated from the reverberation mapping, while the relation of R_{BLR} and AGN luminosity is assumed to hold for all luminosities and redshifts (Kaspi et al. 2000, 2005).

CHAPTER 6

Discussion of the papers

This chapter presents a short discussion of the results of the papers included in Thesis.

6.1 Near-infrared observations of quasar host galaxies

Paper I: The luminous host galaxies of high redshift BL Lac objects: Kotilainen, J.K., Hyvönen, T., Falomo, R., Astron. Astrophys., 440, 831-843 (2005)

In this paper we present the first sizable sample of near-infrared K_s-band imaging of 13 intermediate redshift ($0.6 < z < 1.3$) BL Lac objects to characterize the properties of their host galaxies. The dataset allows us to study the evolution of BL Lac host galaxies from the present epoch up to $z \sim 1$.

Our near-infrared imaging supports previous results obtained in optical wavelengths, that the host galaxies of BL Lac objects are large ($r_e \sim 7$ kpc*)* and luminous galaxies, which are well represented by a de Vaucouleurs $r^{1/4}$ surface brightness law. Their average bulge scale length is similar to that of low redshift BL Lac hosts indicating lack of evolution in the structure of the galaxies. On the other hand, the host galaxies at intermediate redshifts were found to be very luminous with average K_s-band absolute magnitude $M_{\rm Ks} = -27.9 \pm 0.7$, ~3 mag brighter than L^* galaxies, and ~1 – 1.5 mag brighter than low redshift brightest cluster galaxies. Furthermore, the luminosities are in agreement with those of flat spectrum radio quasars at similar redshift range. The intermediate redshift BL Lac host galaxies appear to be ~2 mag brighter than the hosts at low redshift indicating strong luminosity evolution. They are inconsistent with passive evolution of the host galaxy, requiring a contribution from a relatively recent star formation episode at $z > 0.5$. However, intermediate redshift BL Lac objects are more luminous than their low redshift counterparts over a wide wavelength range, from radio to X-rays, indicating that it is not possible to directly compare the properties of objects at different redshift. Because they belong to different regions of the BL Lac luminosity function, and because of flux-limited surveys, only the brightest objects are observed at higher redshifts, thus inducing a strong selection effect. Unlike in their low redshift counterparts, the nuclear luminosities of intermediate redshift BL Lac objects correlate with the host luminosity. This correlation, combined with selection effects, suggests that the most luminous BL Lac objects are preferentially found in the most luminous galaxies and, consequently, no strong luminosity evolution would be needed.

The nuclear brightness and the nuclear-to-host luminosity ratio of the studied BL Lac hosts are much higher than those of low redshift BL Lac hosts, but similar to flat and steep spectrum radio quasars at the same redshift. The high nuclear brightness

indicates selection effects in the sample originating either from high luminosity of the nucleus or from strong Doppler boosting. Intermediate redshift BL Lacs appear to radiate with a wide range of power with respect to their Eddington luminosity, that is intermediate between the low level observed in nearby BL Lac objects, and the higher level found in luminous radio-loud quasars.

Paper II: The host galaxies of radio-quiet quasars at 0.5 < z < 1.0:
Hyvönen**,** T**.**, Kotilainen, J.K., Örndahl, E., Falomo, R., & Uslenghi, M.
Astron. Astrophys., 462, 525-533 (2007)

This paper presents the first reasonably sized sample of 15 intermediate redshift ($0.5 < z < 1$) radio-quiet quasar (RQQ) host galaxies imaged in the near-infrared *H*-band. The host galaxies of RQQs were found to be luminous (the average *H*-band absolute magnitude $M_H = -26.3 \pm 0.6$) and large elliptical galaxies (scale length $r_e \sim 11$ kpc) represented by de Vaucouleurs $r^{1/4}$ surface brightness law. This supports the previous results that, despite of their radio emission properties, bright quasars are mostly hosted by elliptical galaxies. The hosts of intermediate redshift RQQs appear to be ~1 mag brighter than low redshift L^* galaxies, but they are ~0.5 mag fainter than the hosts of radio-loud quasars (RLQ) at similar redshift range. Furthermore, by comparing the luminosities of the RQQ and RLQ hosts from present epoch up to $z \sim 2$, our result confirms that RQQ hosts are systematically ~0.5 mag fainter over a wide redshift range. However, they are consistent with the model in which the stellar population has been formed at high redshifts and evolved passively since that. Moreover, intermediate redshift RQQs appear to have fainter nuclear luminosity than FSRQs and SSRQs at similar redshift range indicating that the central engines of RQQs are less powerful than those of RLQs.

The black hole masses of RQQs were also estimated by using the relation $\log(M_{BH}/M_\odot) = -0.5(\pm0.02)M_R - 2.96(\pm0.48)$ (McLure & Dunlop 2002, Marconi & Hunt 2003). The average black hole mass for RQQs was found to be $\log(M_{BH}/M_\odot)_{RQQ} = 8.92 \pm 0.29$ that is consistent with those of low redshift RQQs, but smaller than the average black hole mass of RLQs ($\log(M_{BH}/M_\odot)_{RLQ} = 9.22 \pm 0.61$). The difference in black hole masses may reflect a fundamental difference between the central engines of RQQs and RLQs, supporting the view that the black hole mass may be a crucial parameter to the triggering of radio emission.

6.2 Multicolor imaging of low redshift BL Lac objects

Paper III: The stellar content of low redshift BL Lacertae host galaxies from multicolor imaging: Hyvönen, T., Kotilainen, J.K., Falomo, R., Örndahl, E. & Pursimo, T., Astron. Astrophys., 476, 723-734 (2007)

In this paper we present multicolor *UBV*-band imaging of low redshift ($z < 0.3$) BL Lac

host galaxies. *B*-band imaging was obtained for 18 objects together with a subset in the *U*- and *V*-band. The hosts were previously resolved in the *R*- and *H*-bands allowing us to use *UBVRH*-multicolor data to derive the blue-red-near-infrared colors and color gradients of the BL Lac host galaxies, and compare them with the ellipticals with and without nuclear activity.

The host galaxies were found to be luminous and large ellipticals represented well by de Vaucouleurs $r^{1/4}$ surface brightness law with average *B*-band absolute magnitude $M_B = -21.6 \pm 0.7$, and the scale length $r_e \sim 7$ kpc. The *B*-band Kormendy relation of BL Lac hosts is in agreement with that of inactive ellipticals and radio galaxies indicating structural and dynamical similarities between all massive bulges. This suggests that all massive bulges can experience nuclear activity without significant perturbations of their dynamical structure. However, BL Lac hosts do not follow the integrated blue/near-infrared color-magnitude relation for inactive ellipticals, but their $B-H$ color distribution is significantly wider (average $B-H = 3.5 \pm 0.5$) with steeper color gradients than those of inactive ellipticals. Blue colors are most likely caused by a young stellar population component indicating a link between star formation, induced possibly by an interaction or merging event, and the onset of the nuclear activity. The existence of the young stellar population is also supported by stellar population modeling which indicates a presence of intermediate age (~2 Gyr) stellar population in the majority of the BL Lac hosts. This is consistent with the intermediate age stellar component of low redshift radio galaxies obtained by a recent optical spectroscopic study. However, the BL Lac hosts are smooth ellipticals without any peculiar morphologies, such as tidal tails, indicating a recent interaction. The lack of strong signs of interaction suggests a significant time delay between the star formation event, and the start of the nuclear activity.

6.3 Near-infrared spectroscopy of low redshift radio galaxies

Paper IV: The stellar content of low redshift radio galaxies from near-infrared spectroscopy: Hyvönen, T., Kotilainen, J.K., Reunanen, J.,Falomo, R.
Astron. Astrophys., accepted

We observed near-infrared *HK*-band spectra of low redshift radio galaxies to compare the near-infrared properties of radio galaxies with those of inactive ellipticals, and furthermore, to produce the first *HK*-band spectra for low redshift radio galaxies. To study the stellar populations of host galaxies, the analysis of spectral indices is the most suitable way to proceed. In fact, near-infrared region contains many diagnostic stellar absorption features, namely SiI(1.589 μm), CO(6-3)(1.619 μm) in the *H*-band, and NaI(2.207 μm), CaI(2.263 μm) and CO(2-0)(>2.29 μm) bandhead in the *K*-band, that are especially useful for tracing a relatively recent star formation in galaxies. For instance, CO(2-0) bandhead is very strong in young (10 – 100 Myr) giant and supergiant stars and strong in cool asymptotic giant branch stars (100 Myr – 1 Gyr), while it is weaker in older stellar population. To characterize their stellar properties, the

five near-infrared stellar absorption features were measured for both radio galaxy and inactive elliptical galaxy samples.

It was found that on average the EW of CO(2.29) feature of radio galaxies is somewhat greater than that of inactive ellipticals. Most likely, EW(CO2.29) is not significantly affected by dilution suggesting that the ellipticals containing AGN are actually in a different evolutionary stage than their inactive counterparts. This is also supported by comparing other indices, such as CaI and NaI, with each other.

Furthermore, to characterize the age of the populations, the theoretical time-evolution curves of the EWs were calculated by a stellar synthesis model, and fitted with the observed ones. The measured indices are in agreement with two-component stellar population, containing both old and intermediate age components. However, it is worth to note that the age estimates may also be affected by metallicity effect. The results are consistent with previous optical spectroscopic studies, which have shown evidence on the intermediate age (~2 Gyr) stellar populations of nearby radio galaxies, and also in some of the inactive ellipticals. Radio galaxies, however, appear to contain a slightly older stellar population that are found in late-type starburst galaxies suggesting that radio galaxies have undergone an enhanced star formation earlier than starburst galaxies.

Bibliography

Adams, T.F. 1977, *Astrophys. J. Suppl*., 33, 19
Ali, B., Carr, J., DePoy, D., Frogel, J. & Sellgren, K. 1995, *Astron. J.*, 110, 2415
Alonso-Herrero, A., Rieke, M.J., Rieke, G.H. & Shields, J.C. 2000, *Astrophys. J*., 530, 688
Ando, K.J., Love, P.J., Lum, N.A., Gulbransen, D.J., Hoffman, A.W. et al. 2004, *Scientific Detectors for Astronomy, The Beginning of a New Era,* ed. Amico, P., Beletic, J.W., Belectic, J.E, 300, 11
Antonucci, R. & Miller, J.S. 1985, *Astrophys. J*., 297, 621
Arnal, E., Duronea, N. & Testori, J. 2008, *Astron. Astrophys*., 486, 807
Ascasibar, Y., Yepes, G., Gottlöber, S. & Muller, V. 2002, *Astron. Astrophys*., 387, 396
Bahcall, J.N., Kirhakos, S., Saxe, D.H. & Schneider, D.P. 1997, *Astrophys.J*., 479, 642
Baldwin, J.A. 1977, *Astrophys. J*., 214, 679
Baldwin, J.A., Ferland, G.J., Korista, K.T., Hamann, F. & Dietrich, M. 2003, *Astrophys. J*., 582, 590
Balick, B. & Brown, R.L. 1974, *Astrophys. J*., 194, 265
Balogh, M.L., Schade, D., Morris, S.L., Yee, H.K.C., Carlberg, R.G. & Ellingson, E. 1998, *Astrophys. J*., 504, 75
Barth, A.J., Ho, L.C, Rutledge, R.E. & Sargent, W.L.W. 2004, *Astrophys. J*., 607, 90
Barthel, P.D. 1989, *Astrophys. J*., 336, 606
Becker, R.H., White, R.L. & Helfand, D.J. 1995, *Astrophys. J*., 450, 559
Becklin, E.E., Tielens, A.G.G.M. & Callis, H.H.S. 2007, *Advances in Space Research*, 40, 644
Beckmann, V., Soldi, S., Schrader, C.R., Gehrels, N. & Produit, N. 2006, *Astrophys. J*., 652, 126
Bennert, N., Canalizo, G., Jungwiert, B., Stockton, A., Schweizer, F. et al. 2008, *Astrophys. J*., 677, 846
Best, P.N. 2004, *Mon. Not. R. Astron. Soc*., 351, 70
Blandford, R.D. & Rees, M.J. 1974, *Mon. Not. R. Astron. Soc.*, 169, 395
Blanford, R.D. & Znajek, R.L. 1977, *Mon. Not. R. Astron. Soc*., 179, 433
Blandford, R.D. 1990, in *Active Galactic Nuclei*, eds. T.J.-L. & M. Mayor, Berlin:Springer, Saas-Fee Advance Course 20, 328
Boroson, T.A., Oke, J.B. & Green, R.F. 1982, *Astrophys. J.*, 263, 32
Boroson, T.A., Persson, S.E. & Oke, J.B. 1985, *Astrophys. J.*, 293, 120
Botti, I, Lira, P., Netzer, H., Kaspi, S., Maza, J. et al. 2008, arXiv0805.4664
Boyle, B.J., Fong, R., Shanks, T. & Peterson, B.A. 1990, *Mon. Not. R. Astron. Soc*., 243, 1
Boyle, B.J., Griffiths, R.E., Shanks, T., Stewart, G.C. & Georgantopoulos, I. 1993, *Mon. Not. R. Astron. Soc*., 260, 49
Boyle, B.J. 2001, *Advanced Lectures on the Starburst-AGN Connection*, (ed. I. Aretxaga, D. Kunth, R. Mujica), Singapore: World Scientific
Bower, R.G., Lucey, J.R. & Ellis, R.S. 1992a, *Mon. Not. R. Astron. Soc*., 254, 589
Bower, R.G., Lucey, J.R. & Ellis, R.S. 1992b, *Mon. Not. R. Astron. Soc*., 254, 607

Bower, R.G., Benson, A.J., Malbon, R., Helly, J.C., Frenk, C.S. et al. 2006, *Mon. Not. R. Astron. Soc*., 370, 645
Bressan, A., Granato, G.L. & Silva, L. 1998, *Astron. Astrophys.*, 332, 135
Bressan, A., Falomo, R., Valdes, J.R. & Rampazzo, R. 2006, *Astrophys. J*., 645, L101
Bridle, A.H., Hough, D.H., Lonsdale, C.J., Burns, J.O & Laing, R.A. 1994, *Astron. J*., 108, 766
Bruzual, G. & Charlot, S. 2003, *Mon. Not. R. Astron. Soc*., 344, 1000
Byrd, G. & Valtonen, M. 2001, *Astron. J*., 121, 2943
Calzetti, D., Kinney, A.L. & Storchi-Bergmann, T., 1994, *Astrophys. J.*, 429, 582
Canalizo, G. & Stockton, A. 2001, *Astrophys. J*., 555, 719
Capaccioli, M.,Caon,N. & D'Onofrio,M. 1992, *Mon.Not. R.Astron.Soc*.,259,323
Cardelli, J.A., Clayton, G.C. & Mathis, J.S. 1989, *Astrophys. J.*, 345, 245
Cavaliere, A. & Vittorini, V. 2000, *Astrophys. J*., 543, 599
Cesarsky, C.J. & Salama, A., 2006, *ISO Science Legacy*, Ed. Cesarsky, C.J. European Sothern Observatory, Garching, Munich, Salama, A., European Space Agency, Madrid, Spain
Cid Fernandez, R., Gonzalez Delgado, R.M., Schmitt, H.,Storchi-Bergmann,T., Martins, L.P., et al. 2004, *Astrophys. J*., 605, 105
Combes, F. 2005, [astro-ph/0505463]
Corbin, M.R. 2000, *Astrophys. J*., 536, L73
Crenshaw, D.M., Kraemer, S.B. & Gabel, J.R. 2003, *Astron. J.*, 126, 1690
Crenshaw, D.M. & Kraemer 2007, *Astrophys. J*., 659, 250
Croom, S.M., Smith, R.J., Boyle, B.J., Shanks, T., Miller, L. et al. 2004, *Mon. Not. R. Astron. Soc.,* 349, 1397
Daddi, E., Renzini, A., Pirzkal, N., Cimatti, A., Malhotra, S. et al. 2005, *Astrophys. J*., 626, 680
Dahari, O. 1984, *Astron. J*., 89, 966
de Grijp, M.H.K., Keel, W.C., Miley, G.K., Goudfrooij, P. & Lub, J. 1992, *Astron. Astrophys. Suppl*., 96, 389
De Lucia, G., Springel, V., White, S.D.M., Croton, D., Kauffmann, G. 2006, *Mon. Not. R. Astron. Soc.*, 366, 499
de Vaucouleurs, G., 1948, *Ann. Astrophys*., 11, 247
Di Matteo, T., Croft, R.A.C., Springel, V. & Hernquist, L. 2004, *Astrophys. J*., 610, 80
Djorgovski, S. & Davis, M. 1987, *Astrophys. J*., 313, 59
Dressler, A. 1980, *Astrophys. J*., 236, 351
Dressler, A., Lynden-Bell, D., Burstein, D., Davies, R.L., Faber, S.M., et al. 1987, *Astrophys. J*., 313, 42
Dunlop, J.S. & Peacock, J.A. 1990, *Mon. Not. R. Astron. Soc.*, 247, 19
Dunlop, J.S., McLure, R.J., Kukula, M.J., Baum, S.A., O'Dea, C.P. & Hughes, D.H. 2003, *Mon. Not. R. Astron. Soc*., 340, 1095
Dunham, E.W. 1995, *Astronomical Society of the Pacific Conference Series,* 73, 679
Eckart, A. & Genzel, R. 1997, *Mon. Not. R. Astron. Soc.*, 284, 576
Ellingson, E., Yee, H.K.C. & Green, R.F. 1991, *Astrophys. J*., 371, 49
Elvis, M. 2000, *Astrophys. J*., 545, 63
Falomo, R. & Kotilainen, J.K. 1999, *Astron. Astrophys*., 352, 85

Falomo, R., Carangelo, N. & Treves, A. 2003, *Mon. Not. R. Astron. Soc*., 343, 505
Falomo, R., Kotilainen, J.K., Pagani, C., Scarpa, R. & Treves, A. 2004, *Astrophys. J*., 604, 495
Falomo, R., Kotilainen, J.K., Scarpa, R. & Treves, A. 2005, *Astron. Astrophys*., 434, 469
Falomo, R., Treves, A., Kotilainen, J.K., Scarpa, R. & Uslenghi, M. 2008, *Astrophys. J*., 673, 694
Fan, X. 1999, *Astron. J*., 117, 2528
Fanaroff, B.L. & Riley, J.M. 1974, *Mon. Not. R. Astron. Soc.,* 167, L31
Fendt, C., 1997, *Astron. Astrophys*., 319, 1025
Ferguson, J.W., Korista, K.T., & Ferland, G.J.1997, *Astrophys. J. Suppl. Ser.*, 110, 287
Ferrarese, L. & Merritt, D. 2000, *Astrophys. J*., 539, L91
Ferrarese, L. 2002, *Astrophys. J*., 578, 90
Ferrarese, L. 2006, *Joint Evolution of Black Holes and Galaxies*, (ed. M. Colpi et al., Taylor & Francis Group)
Filippenko, A.V. & Ho, L.C. 2003, *Astrophys. J*., 588, L13
Finger, G., Dorn, R.J., Mehrgan, H., Meyer, M., Moorwood, A.F.M. & Steigmeier, J. 2004, *Scientific Detectors for Astronomy, The Beginning of a New Era,* ed. Amico, P., Beletic, J.W., Belectic, J.E., 300, 497
Fioc, M. & Rocca-Volmerange, B. 1997, *Astron. Astrophys*., 326, 950
Floyd, D.J.E., Kukula, M.J., Dunlop, J.S., McLure, R.J., Miller, L., et al. 2004, *Mon. Not. R. Astron. Soc*., 355, 196
Ford, H.C., Harms, R.J., Tsvetanov, Z.I., Hartig, G.F., Dressel, L.L. et al. 1994, *Astrophys. J*., 435, 27
Franceschini, A., Hasinger, G., Miyaji, T. & Malquori, D. 1999, *Mon. Not. R. Astron. Soc.*, 310, L5
Franceschini, A., Bassani, L., Cappi, M., Granato, G.L., Malaguti, G. et al. 2000, *Astron. Astrophys.*, 353,910
Freeman, K.C., 1970, *Astrophys. J*., 160, 811
Gabor, J.M., Impey, C.D., Jahnke, K., Simmons, B.D., Trump, J.R. et al. 2009, *Astrophys. J*., 691, 705
Gardner, J.P., Shaples, R.M., Frenk, C.S. & Carrasco,B.E. 1997, *Astrophys. J.*, 480, L99
Ghez, A.M., Morris, M., Becklin, E., Tanner, A. & Kremenek, T. 2000, *Nature*, 407, 349
Gilli, R., Comastri, A. & Hasinger, G. 2007, *Astron. Astrophys.*, 463, 79
Gioia, I.M., Maccacaro, T., Schild, R.E., Wolter, A., Stocke, J.T. et al. 1990, *Astrophys. J. Suppl. Ser.*, 72, 567
Granato, G.L., De Zotti, G., Silva, L., Bressan, A. & Danese, L. 2004, *Astrophys. J.*, 600, 580
Green, A.R., McHardy, I.M. & Lehto, H.J. 1993, *Mon. Not. R. Astron. Soc.*, 265, 664
Green, F.R., Williams, T.B. & Morton, D.C. 1978, *Astrophys. J.*, 226, 729
Greenhill, L.J., Gwinn, C.R., Antonucci, R. & Barvainis, R. 1996, *Astrophys. J*., 472, L21
Greenstein, J.L. & Schmidt, M. 1964, *Astrophys. J*., 140, 1

Gregg, M.D., Becker, R.H., White, R.L., Helfand, D.J., McMahon, R.G. & Hook, I.M. 1996, *Astron. J.*, 112, 407
Grogin, N.A., Conselice, C.J., Chatzichristou, E., Alexander, D.M., Bauer, F.E. et al. 2005, *Astrophys. J.*, 627, 97
Govoni, F., Falomo, R., Fasano, G. & Scarpa, R. 2000, *Astron. Astrophys*., 353, 507
Gu, Q. & Huang, J. 2002, *Astrophys. J.* 579, 205
Hamilton, T.S., Casertano, S. & Turnshek. 2002, *Astrophys. J.*, 576, 61
Harms, R.J., Ford, H.C., Tsvetanov, Z.I., Hartig, G.F., Dressel, L.L. et al. 1994, *Astrophys. J.*, 435, L35
Heckman, T.M. 1980, *Astron. Astrophys*., 87, 152
Heckman, T.M., O'Dea, C.P., Baum, S.A. & Laurikainen, E., 1994, *Astrophys. J.*, 428, 65
Hernquist, L. 1989, *Nature*, 340, 687
Hes, R., Barthel, P.D. & Fosbury, R.A. 1993, *Nature*, 362, 326
Hewett, P.C., Foltz, C.B. & Chaffee, F.H. 1995, *Astron. J.*, 109, 1498
Ho, L.C., Filippenko, A.V. & Sargent, W.L.W. 1993, *Astrophys. J.*, 417, 63
Ho, L.C., Filippenko, A.V. & Sargent, W.L.W. 1997, *Astrophys. J.*, 487, 568
Ho, L.C., Feigelson, E.D., Townsley, L.K., Sambruna, R.M., Garmire,G.P. et al. 2001, *Astrophys. J.*, 549, 51
Ho, L.C. 2002, *Astrophys. J.*, 564, 120
Hoyle, F. & Fowler, W.A. 1963, *Mon. Not. R. Astron. Soc.*, 125, 169
Huchra, J. & Burg, R. 1992, *Astrophys. J.*, 393, 90
Hughes, D.H., Kukula, M.J., Dunlop, J.S. & Boroson, T. 2000, *Mon. Not. R. Astron. Soc*., 316, 204
Hutchings, J.B., Janson, T. & Neff, S.G. 1989, *Astrophys. J.*, 342, 660
Häring, N. & Rix, H.-W. 2004, *Astrophys. J.*, 604, L89
Iye, M., Ota, K., Kashikawa, N., Furusawa, H., Hashomoto, T. et al. 2006, *Nature*, 443, 186
Jackson, N. & Browne, I.W. 1990, *Nature*, 343, 43
Jahnke, K. 2002, PhD thesis, Universität Hamburg
Jahnke, K. & Wisotzki, L. 2003, *Mon. Not. R. Astron. Soc*., 346, 304
Jahnke, K., Kuhlbrodt, B. & Wisotzki, L. 2004, *Mon. Not. R. Astron. Soc*., 352, 399
Jaffe, W., Meisenheimer, K., Röttgering, H.J.A., Leinert, Ch., Richichi, A. et al. 2004, *Nature*, 429, 47
Jannuzi, B.T., Smith, P.S. & Elston, R. 1994, *Astrophys. J.*, 428, 93
Jogee, S., Kenney, J.D.P. & Smith, B.J. 1999, *Astrophys. J.*, 526, 665
Johnson, H.L. 1966, *Annu. Rev. Astron. Astrop*., 4, 193
Jörgensen,I., Franx,M. & Kjaergaard,P. 1996, *Mon. Not.R. Astron. Soc*.,280,167
Kaspi, S., Smith, P.S., Neitzer, H., Maoz, D., Jannuzi, B.T. & Giveon, U. 2000, *Astrophys. J.*, 533, 631
Kaspi,S., Maoz, D., Netzer, H.,Peterson, B.M., Vestergaard,M. & Jannuzi, B.T. 2005, *Astrophys. J.*, 629, 61
Kauffmann, G. & Charlot, S. 1998, *Mon. Not. R. Astron. Soc.*, 294, 705
Kauffmann,G., Heckman,T.M., Tremonti,C., Brinchmann,J., Charlot, S. et al. 2003, *Mon. Not. R. Astron. Soc*., 346, 1055

Kauffmann, G. & Hähnelt, M. 2000, *Mon. Not. R. Astron. Soc.*, 311, 576
Kellermann, K.I., Sramek, R., Schmidt, M., Shaffer, D.B. & Green, R. 1989, *Astron. J.*, 98, 1195
Kennefick, J.D., Djorgovski, S.G. & de Carvalho, R.R. 1995, *Astron. J.*, 110, 2553
Keppens, R., Meliani, Z., van der Holst, B. & Casse, F. 2008, *Astron. Astrophys.*, 486, 663
Khachikian, E.Y. & Weedman, D.W. 1974, *Astrophys. J.* 192, 581
Kinney, A.L., Rivolo, A.R., & Koratkar, A.P. 1990, *Astrophys. J.*, 357, 338
Kirhakos, S., Bahcall, J.N., Schneider, D.P. & Kristian, J. 1999, *Astrophys. J.*, 520, 67
Kleinmann, S. & Hall, D. 1986, *Astrophys. J. Suppl. Ser.*, 62, 501
Kormendy, J. 1977, *Astrophys. J.*, 217, 406
Kormendy, J. 1988, *Astrophys. J.*, 325, 128
Kormendy, J. & Djorgovski, S.G., 1989, *Ann. Rev. Astron. Astrophys*., 27, 235
Kormendy, J. & Richstone, D. 1995, *Ann. Rev. Astron. Astrophys*., 33, 581
Kotilainen, J.K., Falomo, R. & Scarpa, R. 1998a, *Astron. Astrophys*., 332, 503
Kotilainen, J.K., Falomo, R. & Scarpa, R. 1998b, *Astron. Astrophys*., 336, 479
Kotilainen, J.K., & Falomo, R. 2000, *Astron. Astrophys*., 364, 70
Kotilainen, J.K. & Falomo, R. 2004, *Astron. Astrophys*., 424, 107
Kotilainen, J.K., Falomo,R., Treves, A. & Uslenghi, M. 2006, *New. Astron. Rev.* 2006, 50, 772
Kotilainen, J.K., Falomo, R., Labita, M., Treves, A. & Uslenghi, M. 2007, *Astrophys. J.*, 660, 1039
Kotilainen, J.K., Falomo, R., Decarli, R., Treves, A., Uslenghi, M. et al. 2009, *Astrophys. J.*, submitted
Kristian, J. 1973, *Astrophys., J.*, 179, L61
Krolik, J.H. & Begelman, M.C. 1988, *Astrophys. J.*, 329, 702
Kuhlbrodt, B., Wisotzki, L. & Jahnke, K., 2004, *Mon. Not. R. Astron. Soc.,* 349, 1027
Kuhlbrodt, B., Örndahl, E., Wisotzki, L. & Jahnke, K. 2005, *Astron. Astrophys*., 439, 497
Kukula, M.J., Dunlop, J.S. Hughes, D.H. & Rawlings, S. 1998, *Mon. Not. R. Astron. Soc.*, 297, 366
Kukula, M.J, Dunlop, J.S., McLure, R.J., Miller, L., Percival, W.J. et al. 2001, *Mon. Not. R. Astron. Soc.,*326, 1533
Labita, M., Treves, A., Falomo, R. & Uslenghi, M. 2006, *Mon. Not. R. Soc*., 373, 551
Laine, S., Shlosman, I., Knapen, J.H. & Peletier, R.F. 2002, *Astrophys. J*., 567, 97
Lancon, A. & Rocca-Volmerange, B. 1992, *Astron. Astrophys. Suppl. Ser.*, 96, 593
Laor, A. 1998, *Astrophys. J*., 505, L83
Laor, A. 2000, *Astrophys. J*., 543, L111
Laurikainen, E. & Salo, H. 1995, *Astron. Astrophys*., 293, 683
Ledlow, M.J. & Owen, F.N. 1996, *Astron. J*., 112, 9
Letawe, G., Magain, P., Courbin, F., Jablonka, P., Jahnke, K. et al 2007, *Mon. Not. R. Astron. Soc*., 378, 83
Li, Z.-Y., Chiueh, T. & Begelman, M.C. 1992, *Astrophys. J*., 394, 459
Longhetti, M., Saracco, P., Severgnini, P., Della Ceca, R., Mannucci, F. et al. 2007, *Mon. Not. R. Astron. Soc*., 374, 614

Lutz, D., Maiolino, R., Moorwood, A.F.M., Netzer, H., Wagner, S.J. et al. 2002, *Astron. Astrophys*., 396, 429
Lynden-Bell, D. 1969, *Nature*, 223, 690
Maciejewski, W. & Sparke, L.S. 2000, *Mon. Not. R. Astron. Soc.*, 313, 745
Madau, P., Pozzetti, L. & Dickinson, M. 1998, *Astrophys. J*., 498, 106
Maiolino, R., Salvati, M., Bassani, L., Dadina, M, della Ceca, R. et al. 1998, *Astron. Astrophys*., 338,781
Maloney, A, & Petrosian, V. 1999, *Astrophys. J*., 518, 32
Mannucci, F., Basile, F., Poggianti, B., Cimatti, A., Daddi, E. et al. 2001, *Mon. Not. R. Astron. Soc.* 326, 745
Maraston, C. 2005, *Mon. Not. R. Astron. Soc*., 362, 799
Marconi, A. & Hunt, L.K., 2003, *Astrophys. J*., 589, L21
Marconi, A., Risaliti, G., Gilli, R., Hunt, L.K., Maiolino, R. et al. 2004, *Mon. Not. R. Astron. Soc*., 351, 169
Markarian, B.E. 1967, *Astrofizika*, 3, 55
Markarian, B.E., Lipovetskii,V.A. & Stepanian, D.A. 1981, *Astroficika*, 17, 619
Martel, A.R., Baum, S.A., Sparks, W.B., Wyckoff, E., Biretta, J.A. et al. 1998, *Astrophys. J. Suppl.*, 122, 81
Martinez-Sansigre, A., Rawlings, S., Lacy, M., Fadda, D., Jarvis, M.J. et al. 2006, *Mon. Not. R. Astron. Soc.*, 370, 1479
McLeod, K.K. & Rieke, G.H. 1994a, *Astrophys. J*., 420, 58
McLeod, K.K. & Rieke, G.H. 1994b, *Astrophys. J*., 433, 528
McLeod, K.K. & Rieke, G.H. 1995, *Astrophys. J*., 454, L77
McLure, R.J., Kukula, M.J., Dunlop, J.S., Baum, S.A., O'Dea, C.P. & Hughes, D.H., 1999, *Mon. Not. R. Astron. Soc*., 308, 377
McLure, R.J. & Dunlop, J.S. 2001a, *Mon. Not. R. Astron. Soc*., 321, 515
McLure, R.J. & Dunlop, J.S. 2001b, *Mon. Not. R. Astron. Soc*., 327, 199
McLure, R.J. & Dunlop, J.S. 2002, *Mon. Not. R. Soc*., 331, 795
McLure, R.J. & Jarvis, M.J. 2004, *Mon. Not. R. Astron. Soc*., 353, 45
Metcalf, R.B. & Magliocchetti, M. 2006, *Mon. Not. R. Astron. Soc*., 365, 101
Mihos, J.C. & Hernquist, L. 1996, *Astrophys. J*., 464, 641
Miller, J.S., Goodrich, G.C. & Matthews, W. 1991, *Astrophys. J*., 378, 47
Miyoshi, M., Moran, J., Herrnstein, J., Greenhill, L., Nakai, N. et al. 1995, *Nature*, 373, 127
Moran, E.C., Barth,A.J., Kay, L.E. & Filippenko, A.V. 2000, *Astrophys. J*., 540, 73
Moran, E.C., Kay, L.E., Davis, M., Filippenko, A.V. & Barth, A.J., 2001, *Astrophys. J*., 556, L75
Mulchaey, J.S. & Regan, M.W. 1997, *Astrophys. J*., 482, L135
Murakami, H., Freund, M.M., Ganga, K., Guo, H., Hirao, T. et al. 1996, *Publ. Astron. Soc. Japan*, 48, 41
Murayama, T. & Taniguchi, Y. 1998, *Astrophys. J*., 497, L9
Nagamine, K., Fukugita, M., Cen, R. & Ostriker, J.P. 2001, *Astrophys. J*., 558, 497
Nakamura, O., Fukugita, M. Yasuda, N., Loveday, J., Brinkmann, J. et al. 2003, *Astron. J*., 125, 1682
Nandra, K., Laird, E.S. & Steidel, C.C. 2005, *Mon. Not. R. Astron. Soc*., 360,39

Neugebauer, G., Habing., H.J., van Duinen, R., Aumann, H.H., Baud, B. et al. 1984, *Astrophys. J.*, 278, 1
Nolan, L.A., Dunlop, J.S., Kukula, M.J., Hughes, D.H., Boroson, T. & Jimenez, R. 2001, *Mon. Not. R. Astron. Soc*., 323, 308
Oke, J.B. & Gunn, J.E. 1974, *Astrophys. J.*, 189, L5
Oliva, E., Origlia, L., Kotilainen, J.K. & Moorwood, A.F.M. 1995, *Astron. Astrophys*., 301, 55
Origlia, L., Moorwood, A.F.M. & Oliva, E. 1993, *Astron. Astrophys*., 280, 536
Orr, M.J. & Browne, I.W. 1982, *Mon. Not. R. Astron. Soc*., 200, 1067
Osterbrock, D.E. & Koski, A.T. 1976, *Mon. Not. R. Astron. Soc*., 176, 61
Osterbrock, D.E. 1981, *Astrophys. J*., 249, 462
Owen, F.N. & Laing, R.A. 1989, *Mon. Not. R. Astron. Soc*., 238, 357
Padovani, P. & Giommi, P. 1995, *Astrophys. J*., 444, 567
Pagani, C., Falomo, R. & Treves, A. 2003, *Astrophys. J*., 596, 830
Pauliny-Toth, I.I.K. & Kellermann, K.I. 1972, *Astron. J.*, 77, 797
Peletier, R., Valentijn, E. & Jameson, R. 1990, *Astron. Astrophys*., 233, 62
Peng, C.Y., Ho, L.C., Impey, C.D. & Rix, H.-W., 2002, *Astron. J*., 124, 266
Peng, C.Y., Impey, C.D., Rix, H.-W., Kochanek, C.S., Keeton, C.R. et al. 2006, *Astrophys. J*., 649, 616
Piccinotti, G., Mushotzky, R.F., Boldt, E.A., Holt, S.S., Marshall, F.E. et al. 1982, *Astrophys. J*., 253, 485
Pier, E.A. & Krolik, J.H. 1992, *Astrophys. J.*, 401, 99
Pier, E.A. & Krolik, J.H. 1993, *Astrophys. J.*, 428, 124
Pier, E.A. & Voit, G.M. 1995, *Astrophys. J.*, 450, 628
Polletta, M., Weedman, D., Hoenig, S., Lonsdale, C.J., Smith, H.E. & Houck, J. 2008, *Astrophys. J*., 675, 960
Portilla, J.G., Rodriguez-Ardila, A. & Tajeiro, J.M. 2008, *RMxAC*, 32, 80
Rafanelli, P., Violato, M. & Baruffolo, A. 1995, *Astron. J.*, 109, 1546
Raimann, D., Storchi-Bergman, T., Quintana, H., Hunstead, R. & Wisotzki, L. 2005, *Mon. Not. R. Astron. Soc*., 364, 1239
Ramirez, S., DePoy, D., Frogel, J., Sellgren, K. & Blum, R. 1997, *Astron. J.*, 113, 1411
Rees, M.J. 1984, *Annu. Rev. Astron. Astrop*., 22, 471
Rees, M.J., Phinney, E.S., Begelman, M.C. & Blandford, R.D. 1982, *Nature*, 295, 17
Reunanen, J., Kotilainen, J.K. & Prieto, M.A. 2002, *Mon. Not. R. Astron. Soc.*,331, 154
Reunanen, J., Kotilainen, J.K. & Prieto, M.A. 2003, *Mon. Not. R. Astron. Soc.*, 343,192
Reyes, R., Zakamska, N.L.,Strauss, M.A., Green, J., Krolik, J.H. et al. 2008, *Astron. J*., 136, 2373
Richards, G.T., Fan, X., Schneider, D.P., Van den Berk, D.E., Strauss,M.A. et al. 2001, *Astron. J*., 121, 2308
Ridgway, S.E., Heckman, M., Calzetti, D. & Lehnert,M. 2001, *Astrophys. J*., 550, 122
Risaliti, G., Maiolino, R. & Salvati, M. 1999, *Astrophys. J*., 522, 157
Rodriguez-Ardila, A., Viegas, S.M., Pastoriza, M.G. & Prato, L. 2002, *Astrophys. J*., 579, 214
Romanishin, W. & Hintzen, P. 1989, *Astrophys. J*., 341, 41
Rush, B., Malkan, M.A. & Edelson, R.A. 1996, *Astrophys. J*., 473, 130

Salpeter, E.E. 1964, *Astrophys. J.*, 140, 796
Sanchez, S., Jahnke, K., Wisotzki, L., McIntosh, D.H., Bell, E.F. et al. 2004, *Astrophys. J.*, 614, 586
Sanders, D.B., Phinney, E.S., Neugebauer, G., Soifer, B.T. & Matthews, K. 1989, *Astrophys. J.*, 347, 29
Sazonov, S., Revnivtsev, M., Krivonos, R., Churazov, E. & Sunyaev, R. 2007, *Astron. Astrophys*., 462, 57
Schade, D., Boyle, B. & Letawski, M. 2000, *Mon. Not. R. Astron. Soc*., 315,498
Scharwächter, J., Eckart, A., Pfalzer, S., Zuther, J., Krips, M. & Straubmeier, C. 2004, *Astron. Astrophys*., 414, 497
Schulz, A., Henkel, C., Muders, D., Mao, R.Q., Röllig, M. & Mauersberger, R. 2007, *Astron. Astrophys*., 466, 467
Schmidt, M. 1963, *Nature*, 197, 1040
Schmitt, H.R. 2001, *Astron. J.*, 122, 2243
Schmitt, H.R., Antonucci, R., Ulvestad, J.S., Kinney, A.L., Clarke, C.J. & Pringle, J.E. 2001, *Astrophys. J.*, 555, 663
Schramm, M., Wisotzki, L. & Jahnke, K. 2008, *Astron. Astrophys*., 478, 311
Schödel, R., Eckart, A., Alexander, T., Merritt, D., Genzel, R. et al. 2007, *Astron. Astrophys*., 469, 125
Schödel, R., Ott, T., Genzel, R., Hofmann, R., Lehnert, M. et al. 2002, *Nature*, 419, 694
Sersic, J.-L., 1968, *Atlas de Galaxias Australes*, Observatorio Astronomico de Cordoba
Seyfert, C. 1943, *Astrophys. J.*, 97, 28
Shankar, F., Weinberg, D.H. & Miralda-Escude, J., 2009, *Astrophys. J.*, 690, 20
Shields, G.A. 1999, *Publ. Astron. Soc. Pacific*, 111, 661
Shlosman, I., Frank, J. & Begelman, M.C. 1989, *Nature*, 338, 45
Slipher, V.M. 1917, *Lowell Obs. Bull*., 3, 59
Smith, E.P., Heckman, T.M., Bothun, G.D., Romanishin, W. & Balick, B, 1986, *Astrophys. J.*, 306, 64
Soifer, B.T., Sanders, D.B., Neugebauer,G., Danielson,G.E., Lonsdale,C.J. et al. 1986, *Astrophys. J.*, 303, 41
Soifer, B.T., Sanders, D.B., Madore, B.F., Neugebauer, G., Danielson,G.E. et al. 1987, *Astrophys. J.*, 320, 238
Somerville, R.S., Primack, J.R. & Faber, S.M. 2001, *Mon. Not. R. Astron. Soc.*, 320, 504
Springel, V. & Hernquist, L. 2003, *Mon. Not. R. Astron. Soc*., 339, 312
Stocke, J.T., Morris, S.L., Gioia, I.M., Maccacaro, T., Schild, R. & Wolter, A. 1991, *Astrophys. J. Suppl. Ser.*, 76, 813
Storchi-Bergmann, T., Dors, O.L. Jr., Riffel, R.A., Fathi, K., Axon, D.J. et al. 2007, *Astrophsy. J*., 670, 959
Strittmatter, P.A., Hill, P., Pauliny-Toth, I.I.K., Steppe, H., Witzel, A. 1980, *Astron. Astrophys*., 88, L12
Struck, C. 1997, *Astrophys. J. Suppl. Ser.*, 113, 269
Sulentic, J.W., Marziani, P. & Dultzin-Hacyan, D. 2000, *Ann. Rev. Astron. Astrophys*., 38, 521

Söchting, I.K., Clowes, R.G. & Campusano, L.E. 2004 *Mon. Not. R. Astron. Soc.,* 347, 1241
Tacconi, L.J., Genzel, R., Tecza, M., Gallimore, J.F., Downes, D. & Scoville, N.Z. 1999, *Astrophys. J.*, 524, 732
Terlevich, R., Tenorio-Tagle,G., Franco, J. & Melnick, J. 1992, *Mon. Not. R. Astron. Soc.*, 255, 713
Thorne, K.S., Price, R.H. & Macdonald, D.A. ed. 1986, *"Black Holes: The Membrane Paradigm"*, New Haven, Yale Univ Press
Tran, H.D., Miller, J.S. & Kay, L.E. 1992, *Astrophys. J.*, 397, 452
Tran, H.D. 2001, *Astrophys. J.*, 554, L19
Tran, H.D. 2003, *Astrophys. J.*, 583, 632
Urry, C.M. & Padovani, P. 1995, *Publ. Astron. Soc. Pacific*, 107, 803
Uslenghi, M. & Falomo, R. 2007, *in Modeling and Simulation in Science*, ed. V. DiGesu, G. Lo Bosco & M.C. Maccarone (Singapore: World Scientific)
Vazquez, G.A., Carigi, L. & Gonzalez, J.J. 2003, *Astron. Astrophys*., 400, 31
Veilleux, S. & Osterbrock, D.E. 1987, *Astrophys. J. Suppl. Ser.*, 63, 295
Veilleux, S., Kim, D.-C. & Sanders, D.B. 1999, *Astrophys. J.*, 522, 113
Vestergaard, M. 2002, *Astrophys. J.*, 571, 733
Villforth, C., Heidt, J. & Nilsson, K. 2008, *Astron.Astrophys*., 488, 133
Wall, J.V., Wright, A.E. & Bolton, J.G. 1976, *Aust. J. Phys. Astrop. Suppl*., 39, 1
Wandel, A., Peterson, B.M. & Malkan, M.A. 1999, *Astrophys. J.*, 526, 579
Wandel, A. 2002, *Astrophys. J.*, 565, 762
Wallace, L. & Hinkle, K. 1996, *Astrophys. J. Suppl. Ser.*, 107, 312
Wang, J.-M., Li, Y.-R., Wang, J.-C. & Zhang, S. 2008, *Astrophys. J.*, 676, 109
Warren, S.J., Hewitt, P.C. & Osmer, P.S. 1991, *Astrophys. J. Suppl*., 76, 1
Weingartner, J.C. & Draine, B.T. 2001, *Astrophys. J.*, 548, 296
Werner, M.W., Roellig, T.L., Low, F.J., Rieke, G.H., Rieke, M. et al. 2004, *Astrophys. J. Suppl. Ser*, 154, 1
Willott, C.J., Rawlings, S., Blundell, K.M. & Lacy, M. 2000, *Mon. Not. R. Astron. Soc*., 316, 449
Willott, C.J., Rawlings, S., Jarvis, M.J. & Blundell, K.M. 2003, *Mon. Not. R. Astron. Soc*., 339, 173
Willott, C.J., Delorme, P., Omont, A., Bergeron, J, Defosse, X. et al. 2007, *Astron. J*., 134, 2435
Wilson, A.S. & Colbert, E.J.M. 1995, *Astrophys. J.*, 438, 62
Wold, M. Lacy, M., Lilje, P.B. & Serjeant, S. 2001, *Mon. Not. R. Astron. Soc.,* 323, 231
Wurtz, R., Stocke, J.T., Ellingson, E. & Yee, H.K.C. 1997, *Astrophys.J.*,480,547
Yee, H.K.C. & Green, R.F. 1984, *Astrophys. J.*, 400, 30
Yu, Q. & Tremaine, S. 2002, *Mon. Not. R. Astron. Soc*., 335, 965
Zuther, J., Iserlohe, C., Pott, J.-U., Bertram, T., Fischer, S. et al. 2007, *Astron. Astrophys*., 466, 451

Original papers